New $[(\eta^5\text{-}C_5H_5)Ru(N\text{-}N)(PPh_3)][PF_6]$ compounds: colon anticancer activity and GLUT-mediated cellular uptake of carbohydrate-appended complexes

Pedro R. Florindo,[a]* Diane M. Pereira,[b] Pedro M. Borralho,[b] Paulo J. Costa,[c] M. F. M. Piedade,[a,d] Cecília M. P. Rodrigues[b] and Ana C. Fernandes [a]*

[a] Centro de Química Estrutural, Instituto Superior Técnico, Universidade de Lisboa, Av. Rovisco Pais, 1049-001 Lisboa, Portugal.

[b] Research Institute for Medicines (iMed.ULisboa), Faculty of Pharmacy, Universidade de Lisboa, Av. Prof. Gama Pinto, 1649-003 Lisboa, Portugal.

[c] Centro de Química e Bioquímica, DQB, Faculdade de Ciências da Universidade de Lisboa, Campo Grande, 1749-016 Lisboa, Portugal.

[d] Departamento de Química e Bioquímica, Faculdade de Ciências da Universidade de Lisboa, Campo Grande, 1749-016 Lisboa, Portugal.

Electronic Supporting Information

1. Experimental procedures

1.1. *General Procedures*: All experiments were carried out under inert atmosphere (N_2) using standard Schlenk techniques. Commercial reagents were bought from Sigma-Aldrich and used without further purification. Solvents were dried using standard methods.[1] $[(\eta^5\text{-}C_5H_5)Ru(PPh_3)_2Cl]$[2] and 2,2'-bipyridine-4,4'-dicarbonyl dichloride[3] were synthesized according

to previously described procedures. ^{1}H, ^{13}C and ^{31}P NMR spectra were recorded on a Bruker Avance II 400 spectrometer, at probe temperature. ^{1}H and ^{13}C NMR chemical shifts are reported in parts per million (ppm) downfield from the residual solvent peak; ^{31}P NMR spectra are reported in ppm downfield from internal standard (hexafluorophosphate anion, δ = -144.2 ppm). Coupling constants are reported in Hz. Assignments of ^{1}H and ^{13}C NMR spectra were confirmed with the aid of two dimensional techniques ^{1}H, ^{13}C (COSY, HSQC). Microanalyses were performed at Laboratório de Análises do Instituto Superior Técnico, using a Fisons Instruments EA1108 system and data acquisition, integration and handling were performed using the software package Eager-200 (Carlo Erba Instruments), confirming ≥ 95% purity for all biologically tested compounds.

1.2. Synthesis of Ligand **L1**

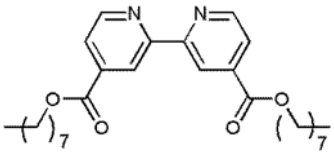

To a shlenck charged with 2,2'-bipyridine-4,4'-dicarbonyl dichloride (470 mg, 1mmol) and 1-octanol (190 µL, 1.2 mmol) was added CH_2Cl_2 (20 mL) and Et_3N (180 µL, 1.2 mmol). The reaction mixture was stirred 24 hours at r.t. and then pumped to dryness. The crude product was purified by column chromatography (eluent: AcOEt/n-hexane 1:9) affording the pure product as a colorless syrup. H = 90%.^{1}H NMR (400 MHz): 0.88 (t, 6H, J = 6.8, $2CH_3$), 1.28-1.46 (comp, 20H, $2(CH_2)_5$), 1.89 (qd, 4H, J = 6.8, $-C\underline{H_2}CH_2O$), 4.39 (t, 4H, J = 6.8, $-CH_2C\underline{H_2}O$), 7.90 (d, 2H, J = 4.8, H5), 8.86 (d, 2H, J = 4.8, H6), 8.94 (s, 2H, H3). ^{13}C NMR (100 MHz): 14.20 (CH_3), 22.8, 26.1, 28.8, 29.3, 29.4, 31.9 ($6CH_2$), 66.2 (CH_2O), 120.7 (C3) 123.4 (C5), 139.2 (C2), 150.2 (C6), 156.7 (C4), 165.4 (CO).

1.3. General procedure for the synthesis of ligands **L1-L4**: To a stirred solution of the corresponding primary alcohol (10 mmol) in pyridine (2 mL) cooled to 0 ºC, was added a solution of TsCl (11 mmol) in dichloromethane (2 mL). The mixture allowed to react for 30 min at 0 ºC, and then for 1 h at r.t. The solvent was then removed, the crude dissolved in toluene and evaporated 3x to eliminate pyridine. The tosylated crude product was dissolved in DMF (5 mL) and NaN_3 (11 mmol) was added. The mixture was then stirred at 100 ºC for 2 h. The solvent was removed under reduced pressure and the crude purified by column chromatography (AcOEt:*n*-hexane), affording the pure azide derivatives. The azide compounds (2 mmol) were dissolved in a mixture of THF (5 mL) and toluene (20 mL). 2-Ethynylpyridine (4 mmol), DIPEA (8 mmol), and CuI (2 mmol) were added to the reaction mixture. After refluxing for 24h, the solvent was removed under reduced pressure and the crude reaction mixture was loaded

on a silica gel column packed with AcOEt/hexane (1:1). The products **L1-L4** were isolated with AcOEt as eluent.

1.3.1. ligand **L5**:

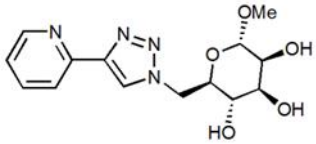

η = 63% (3 steps). ^{1}H NMR (DMSO-d_6, 400 MHz): 2.96 (s, 3H, OCH_3), 3.38-3.48 (comp., 2H, H4' + H5'), 3.60 (br, 1H, H2'), 3.71 (t, 1H, J = 8.8, H3'), 4.49-4.56 (comp., 2H, H6' + H1'), 4.76-4.82 (comp, 2H, H6' + OH), 4.90 (d, 1H, J = 3.6, OH), 5.23 (d, 1H, J = 5.6, OH), 7.33 (br, 1H, $H3_{Pyr}$), 7.88 (t, 1H, J = 7.6, $H4_{Pyr}$), 8.03 (d, 1H, J = 7.2, $H5_{Pyr}$), 8.49 (s, 1H, $H8_{Trzl}$), 8.59 (br, 1H, $H6_{Pyr}$). ^{13}C NMR (DMSO-*d6*, 100 MHz): 51.1 (C6'), 54.2 (OCH_3), 70.2 (C5'), 71.6, 71.7 (C2', C4'), 73.1 (C3'), 99.7 (C1'), 119.4 ($C5_{Pyr}$), 122.9 ($C3_{Pyr}$), 124.2 ($C8_{Traz}$), 137.2 ($C4_{Pyr}$), 147.0 ($C2_{Pyr}$), 149.6 ($C6_{Pyr}$), 150.1 ($C7_{Traz}$).

1.3.2. Ligand **L6**

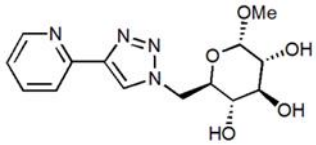

η = 67% (3 steps). ^{1}H NMR (DMSO-d_6, 400 MHz): 2.98 (s, 3H, OCH_3), 3.02-3.06 (m, 1H, H4'), 3.18-3.23 (m, 1H, H2'), 3.40-3.46 (m, 1H, H3'), 3.74-3.79 (m, 1H, H5') 4.48-4.54 (comp., 2H, H6' + H1'), 4.78 (dd, 1H, J = 14.0, 2.4, H6'), 4.83 (d, 1H, J = 6.4, OH), 4.95 (d, 1H, J = 5.2, OH), 5.41 (d, 1H, J = 6.0, OH), 7.33 (br, 1H, $H3_{Pyr}$), 7.86-7.90 (m, 1H, $H4_{Pyr}$), 8.03 (m, 1H, $H5_{Pyr}$), 8.51 (s, 1H, $H8_{Trzl}$), 8.59 (br, 1H, $H6_{Pyr}$). ^{13}C NMR (DMSO-d_6, 100 MHz): 51.1 (C6'), 53.8 (OCH_3), 67.9 (C4'), 70.1 (C2'), 70.7 (C5'), 71.4 (C3'), 101.2 (C1'), 119.4 ($C5_{Pyr}$), 122.9 ($C3_{Pyr}$), 124.2 ($C8_{Traz}$), 137.2 ($C4_{Pyr}$), 147.0 ($C2_{Pyr}$), 149.6 ($C6_{Pyr}$), 150.1 ($C7_{Traz}$).

1.3.3. Ligand **L7**

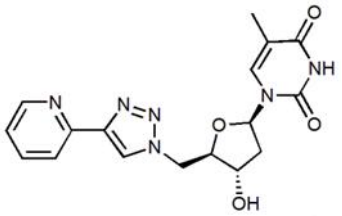

η = 69% (3 steps). ^{1}H NMR (DMSO-d_6, 400 MHz): 1.69 (s, 3H, CH_3), 2.12-2.16 (m, 2H, 2H5'), 4.14-4.16 (m, 1H, H4'), 4.30-4.32 (m, 1H, H3'), 4.73-4.82 (comp., 2H, 2H2'), 5.51-5.54 (m, 1H, -OH), 6.19 (s, 1H, H1'), 7.28-7.34 (comp., 2H, H6 + $H3_{Pyr}$), 7.89 (s, 1H, $H4_{Pyr}$), 8.02 (s, 1H, $H5_{Pyr}$), 8.57 (comp., 2H, $H2_{Pyr}$ + $H8_{Triaz}$), 11.31 (br, 1H, -NH). ^{13}C NMR (DMSO-d_6, 100 MHz):

11.9 (CH_3), 37.9 (C5'), 51.2 (C2'), 70.6 (C3'), 83.7 (C4'), 83.9 (C1'), 109.9 (C5), 119.4 ($C5_{Pyr}$), 122.9 ($C3_{Pyr}$), 124.1 ($C8_{Triaz}$), 135.9 (C6), 137.2 ($C4_{Pyr}$), 147.2 ($C2_{Pyr}$), 149.6, 149.9 ($C7_{Triaz}$ + $C6_{Pyr}$), 150.4 (C2), 163.6 (C4).

1.3.4. Ligand **L8**

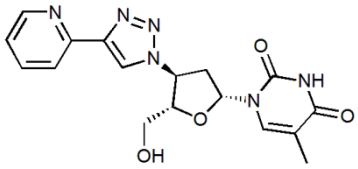

η = 87% (from AZT, 1 step). ^{1}H NMR (DMSO-*d6*, 400 MHz): 1.82 (s, 3H, CH_3), 2.66-2.73 (m, 1H, H5'), 2.80-2.87 (m, 1H, H5'), 3.64-3.75 (comp., 2H, 2H2'), 4.30 (d, 1H, J = 4.4, H4'), 5.29 (t, 1H, J = 5.2, OH), 5.47 (dd, 1H, J = 13.6, 5.6, H3'), 6.46 (t, 1H, J = 6.4, H1'), 7.36 (t, 1H, J = 6.0, $H3_{Pyr}$), 7.85 (s, 1H, H6), 7.90 (t, 1H, J = 7.6, $H4_{Pyr}$), 8.05 (d, 1H, J = 7.6, $H5_{Pyr}$), 8.61 (d, 1H, J = 3.6, $H2_{Pyr}$), 8.83 (s, 1H, $H8_{Triaz}$), 11.36 (br, 1H, -NH). ^{13}C NMR (DMSO-d_6, 100 MHz): 12.3 (CH_3), 37.1 (C5'), 59.5 (C3'), 60.7 (C2'), 83.9 (C1'), 84.4 (C4'), 109.7 (C5), 119.5 ($C5_{Pyr}$), 122.9, 123.1 ($C3_{Pyr}$, $C8_{Triaz}$), 136.93 (C6), 137.3 ($C4_{Pyr}$), 147.5 ($C2_{Pyr}$), 149.6, 149.8 ($C7_{Triaz}$ + $C6_{Pyr}$), 150.5 (C2), 163.7 (C4).

1.4. General procedure for the synthesis of organometallic compounds **1Ru**-**8Ru**:To a Sclenck charged with [(η^5-C_5H_5)Ru(PPh_3)$_2$Cl] (0.2 mmol) and $TlPF_6$ (0.2 mmol) was added CH_2Cl_2 (20 mL), and the mixture was vigorously stirred for 1h, at 40 ºC. The N-N ligand was then added (0.2 mmol) and the mixture was stirred overnight at r.t. The mixture was filtered twice, pumped to dryness, and the crude products were washed with *n*-hexane and Et_2O and then recrystallized by slow diffusion of *n*-hexane or Et_2O in CH_2Cl_2 or acetone solutions.

1.4.1. Compound **1Ru**

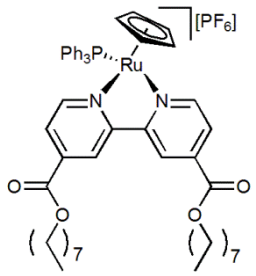

Dark brown; recrystallized from CH_2Cl_2/n-hexane; η = 86%. ^{1}H NMR ($CDCl_3$, 400 MHz): 0.88 (m, 6H, 2CH_3), 1.29-1.42 (comp, 20H, 2$(CH_2)_5$), 1.77-1.84 (m, 4H, -C$\underline{H_2}$$CH_2O$), 4.39 (t, 4H, J = 7.2, -CH_2C$\underline{H_2}$O), 4.85 (s, 5H, η^5-C_5H_5), 6.96-7.09 (comp. 6H, PPh_3) 7.25-7.34 (comp., 9H, PPh_3), 7.79 (d, 2H, J = 5.6, 2H5), 8.21 (s, 2H, 2H3), 9.58 (d, 2H, J = 6.0, 2H6). ^{13}C NMR ($CDCl_3$, 100 MHz): 13.8 (CH_3), 22.0, 25.3, 27.9, 28.5, 28.5, 31.1 (6CH_2), 65.8 (CH_2O), 79.7

(η^5-C_5H_5), 122.6 (C3) 123.3 (C5), 128.5 (d, J_{CP} = 9.6, C_{meta}, PPh_3), 129.8 (C_{para}, PPh_3) 130.2 (d, J_{CP} = 9.4, C_{ortho}, PPh_3), 132.5 (d, J_{CP} = 10.6, C_{ipso}, PPh_3) 136.2 (C2), 155.0 (C2), 156.7 (C4), 163.3 (CO). ^{31}P NMR ($CDCl_3$, 162 MHz): -144.2 (qt, J_{PF} = 712.2, PF_6^-), 50.2 (s, PPh_3). Anal. Calcd. for $C_{51}H_{60}F_6N_2O_4P_2Ru$: C, 58.78; H, 5.80; N, 2.69. Found: C, 59.02; H, 5.65; N, 2.45.

1.4.2. Compound **2Ru**

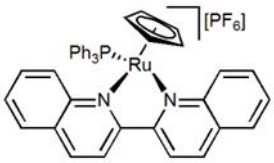

Brown; recrystallized from CH_2Cl_2/n-hexane; η = 92%. ^{1}H NMR (DMSO-d_6, 400 MHz): 5.17 (s, 5H, η^5-C_5H_5), 6.85-6.90 (m, 6H, PPh_3), 7.06-7.09 (m, 6H, PPh_3), 7.21-7.24 (m, 3H, PPh_3), 7.51-7.55 (m, 2H, H7), 7.68-7.72 (m, 2H, H6), 8.04 (d, 2H, J = 8.0, H5), 8.58 (2d, 4H, J = 8.8, H3 + H4), 8.68 (d, 2H, J = 8.8, H8). ^{13}C NMR (DMSO-d_6, 100 MHz): 78.8 (η^5-C_5H_5), 121.3 (C3), 128.2 (C4'), 128.5 (d, J_{CP} = 9.2, C_{meta}, PPh_3), 128.9 (C5), 129.5 (C6), 129.9 (C_{para}, PPh_3), 130.7 (C7), 131.8 (C8), 132.4 (d, J_{CP} = 10.9, C_{ortho}, PPh_3), 133.4 (d, J_{CP} = 39.5, C_{ipso}, PPh_3), 138.0 (C4), 149.4 (C2), 158.7 (C8'). ^{31}P NMR (DMSO-d_6, 162 MHz): -144.2 (qt, J_{PF} = 710.2, PF_6^-), 46.2 (s, PPh_3). Anal. Calcd. for $C_{41}H_{32}F_6N_2P_2Ru$: C, 59.35; H, 3.89; N, 3.38. Found: C, 59.26; H, 3.99; N, 3.08.

1.4.3. Compound **3Ru**

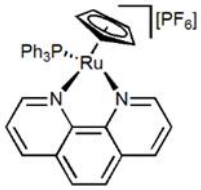

Orange; recrystallized from CH_2Cl_2/n-hexane; η = 79%. ^{1}H NMR (DMSO-d_6, 400 MHz): 4.94 (s, 5H, η^5-C_5H_5), 6.80-6.85 (m, 6H, PPh_3), 7.11-7.15 (m, 6H, PPh_3), 7.24-7.28 (m, 3H, PPh_3), 7.72 (dd, 2H, J = 8.4, 5.2, H3), 7.96 (s, 2H, H5), 8.45 (d, 2H, J = 8.0, H4), 9.73 (d, 2H, J = 5.2, H2). ^{13}C NMR (DMSO-d_6, 100 MHz): 77.9 (η^5-C_5H_5), 124.3 (C3), 127.0 (C5), 128.0 (d, J_{CP} = 9.4, C_{meta}, PPh_3), 129.8, 130.0 (C4' + C_{para}, PPh_3), 130.5 (d, J_{CP} = 42.5, C_{ipso}, PPh_3), 132.2 (d, J_{CP} = 11.0, C_{ortho}, PPh_3), 134.9 (C4), 146.6 (C2), 156.2 (C2'). ^{31}P NMR (DMSO-d_6, 162 MHz): -144.2 (qt, J_{PF} = 710.1, PF_6^-), 52.0 (s, PPh_3). Anal. Calcd. for $C_{35}H_{28}F_6N_2P_2Ru$: C, 55.78; H, 3.74; N, 3.37. Found: C, 55.45; H, 4.05; N, 3.37.

1.4.4. Compound **4Ru**

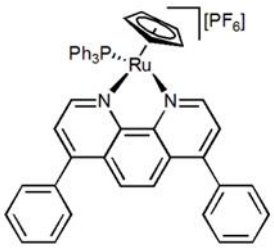

Red; recrystallized from acetone/Et_2O; η = 89%. ^{1}H NMR (DMSO-d_6, 400 MHz): 5.04 (s, 5H, η^5-C_5H_5), 6.92-6.96 (m, 6H, PPh_3), 7.18-7.21 (m, 6H, PPh_3), 7.56-7.66 (comp., 10H, 2Ph), 7.71 (d, 2H, J = 5.6, H3), 7.78 (s, 2H, H5), 9.73 (d, 2H, J = 5.2, H2). ^{13}C NMR (DMSO-d_6, 100 MHz): 78.3 (η^5-C_5H_5), 124.4 (C3), 124.9 (C6), 127.4 (C4'), 128.1 (d, J_{CP} = 9.5, C_{meta}, PPh_3), 129.0, 129.3, 129.8 (Ph) 129.9 (C_{para}, PPh_3), 130.5 (d, J_{CP} = 41.2, C_{ipso}, PPh_3), 132.3 (d, J_{CP} = 10.9, C_{ortho}, PPh_3), 135.4 (Ph), 146.5 (C4), 147.1 (C2), 155.8 (C2'). ^{31}P NMR (DMSO-d_6, 162 MHz): -144.2 (qt, J_{PF} = 712.0, PF_6^-), 51.7 (s, PPh_3). Anal. Calcd. for $C_{47}H_{36}F_6N_2P_2Ru$: C, 62.32; H, 4.01; N, 3.09. Found: C, 62.08; H, 3.88; N, 2.90.

1.4.5. Compound **5Ru**

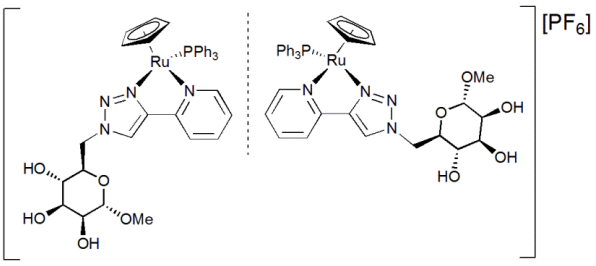

Yellow; recrystallized from CH_2Cl_2/n-hexane; η = 81%. Anal. Calcd. for $C_{37}H_{38}F_6N_4O_5P_2Ru$: C, 49.61; H, 4.28; N, 6.25. Found: C, 49.30; H, 4.49; N, 6.50.

1.4.6. Compound **6Ru**

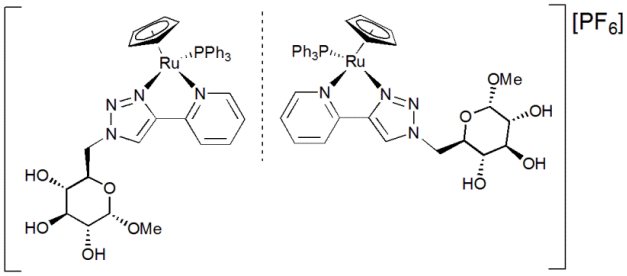

Yellow; recrystallized from CH_2Cl_2/n-hexane; η = 79%. Anal. Calcd. for $C_{37}H_{38}F_6N_4O_5P_2Ru$: C, 49.61; H, 4.28; N, 6.25. Found: C, 49.77; H, 4.35; N, 6.55.

1.4.7. Compound **7Ru**

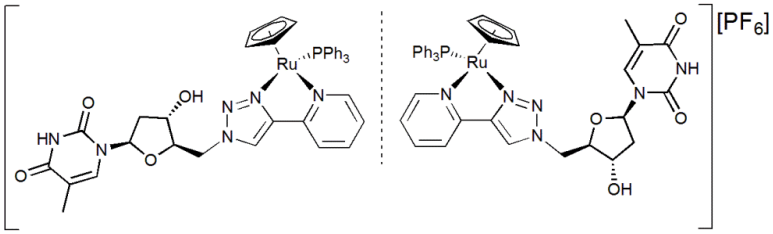

Reddish orange; recrystallized from CH_2Cl_2/n-hexane; η = 83%. Anal. Calcd. for $C_{40}H_{38}F_6N_6O_4P_2Ru$: C, 50.90; H, 4.06; N, 8.90. Found: C, 50.78; H, 4.39; N, 8.76.

1.4.8. Compound **8Ru**

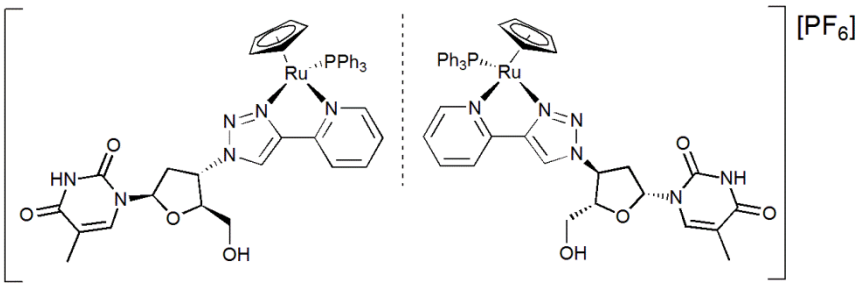

Yellow; recrystallized from CH_2Cl_2/n-hexane; η = 77%. Anal. Calcd. for $C_{40}H_{38}F_6N_6O_4P_2Ru$: C, 50.90; H, 4.06; N, 8.90. Found: C, 51.01; H, 4.36; N, 9.24.

1.4.9. [TM34][PF_6]: Orange; recrystallized from CH_2Cl_2/n-hexane; η = 87%. Anal. Calcd. for $C_{33}H_{28}F_6N_2P_2Ru$: C, 54.32; H, 3.87; N, 3.84. Found: C, 53.99; H, 4.16; N, 3.91.

2. Copies of ^{1}H, ^{13}C and ^{31}P NMR spectra

2.1. Ligand **L1**

2.1.1. ^{1}H NMR ($CDCl_3$, 400 MHz):

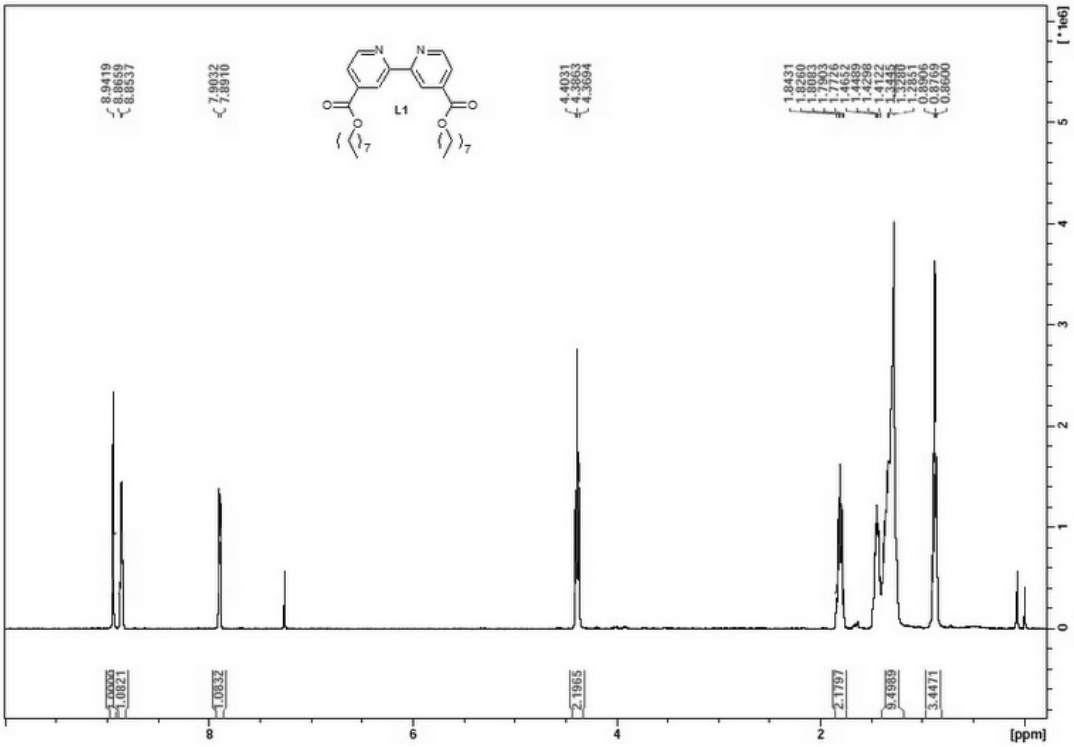

2.1.2. ^{13}C NMR ($CDCl_3$, 100 MHz):

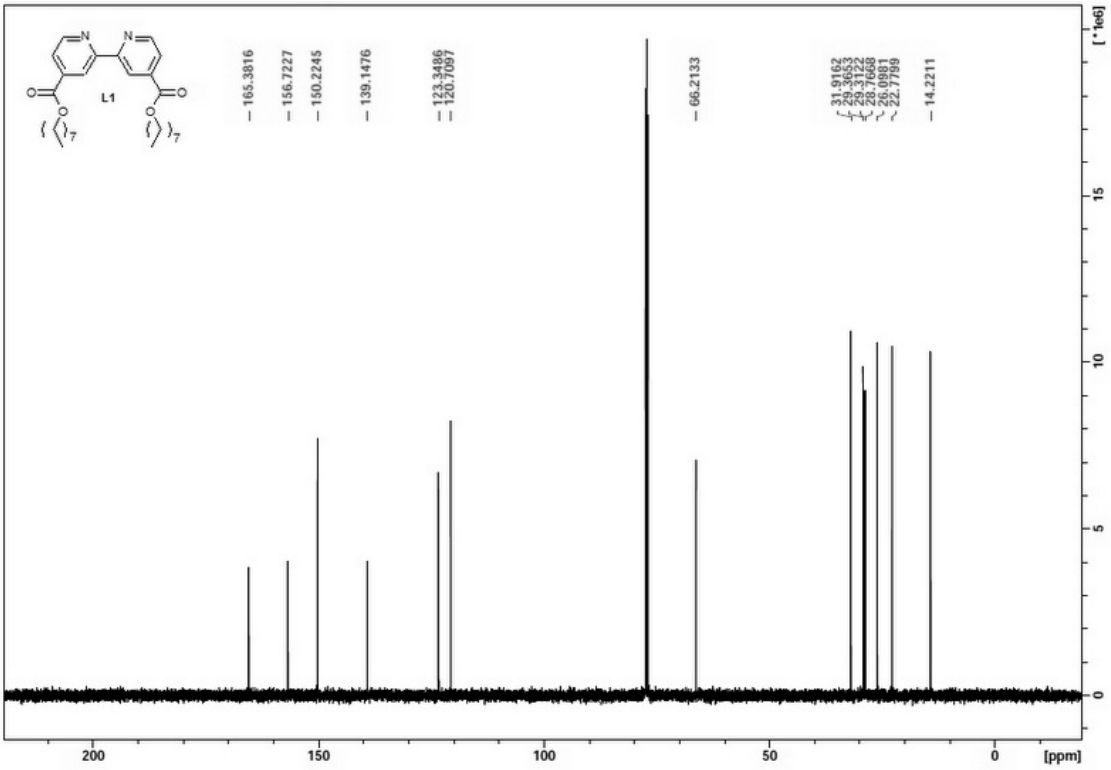

2.2. Ligand **L5**

2.2.1. ^{1}H NMR (DMSO-d_6, 400 MHz):

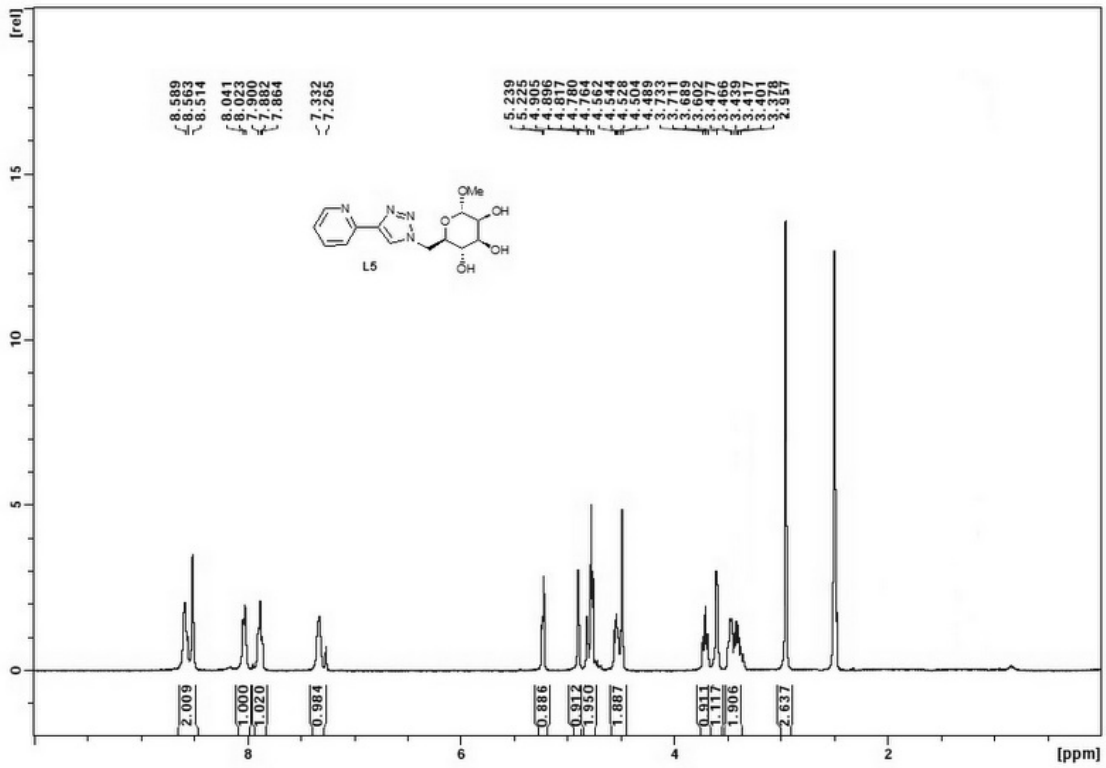

2.2.2. ^{13}C NMR (DMSO-d_6, 100 MHz):

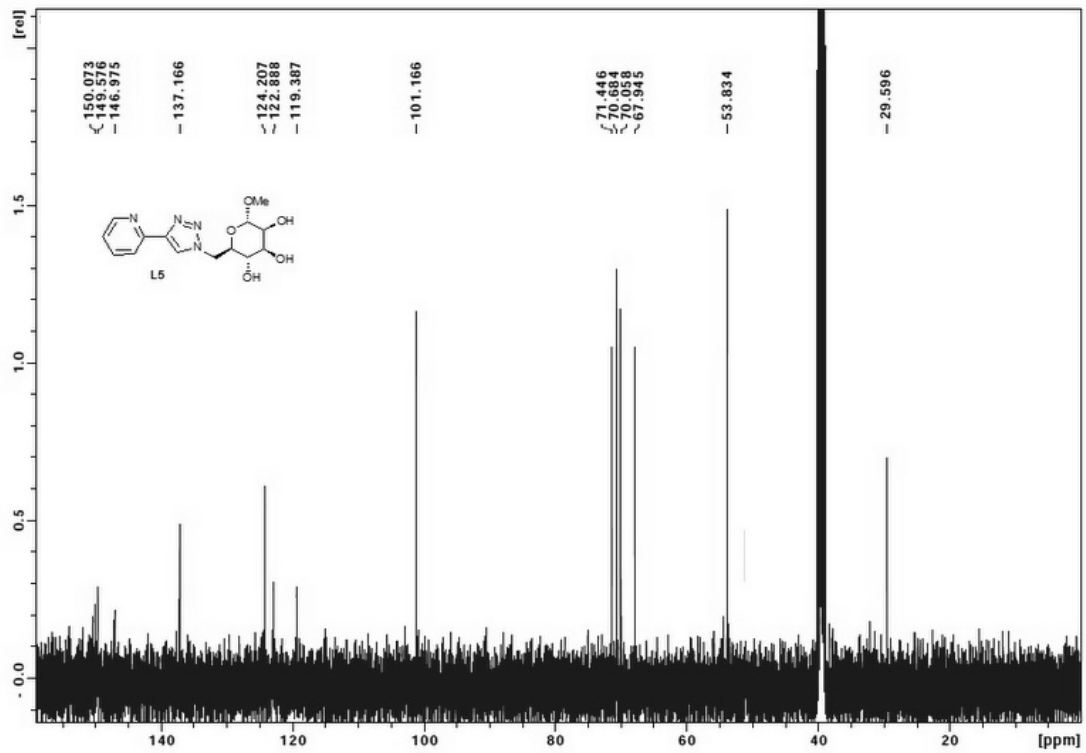

2.3. Ligand **L6**

2.3.1. ^{1}H NMR (DMSO-d_6, 400 MHz):

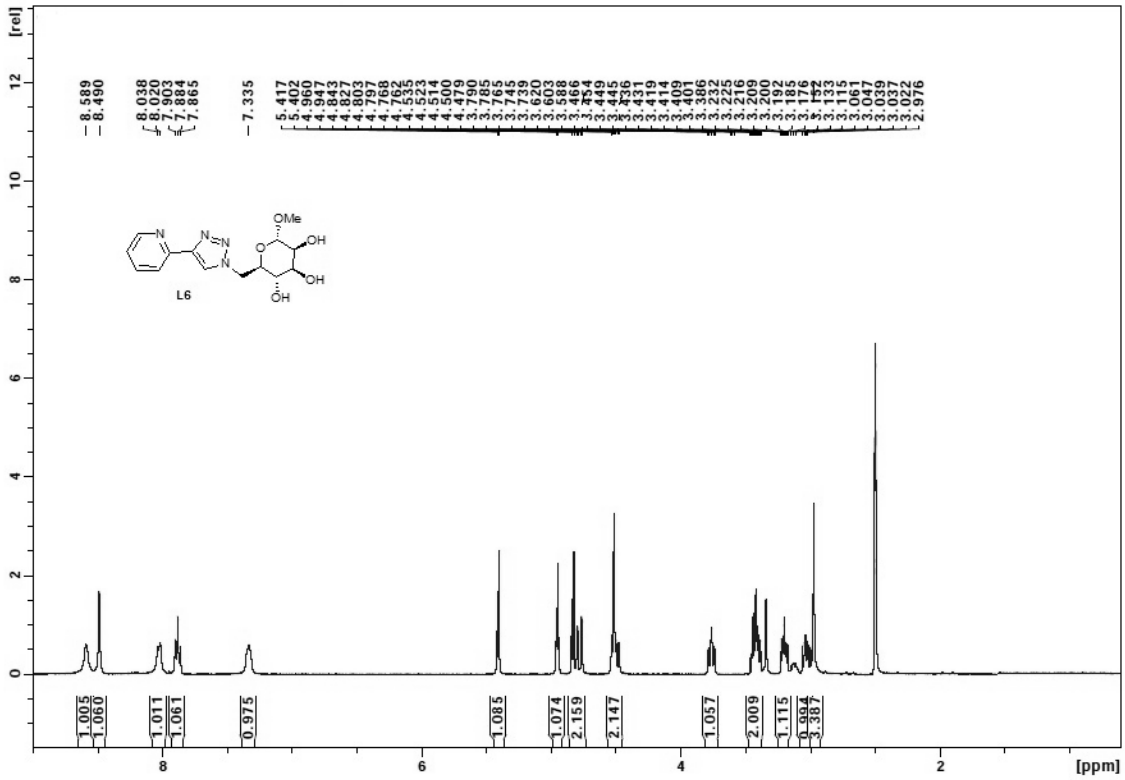

2.3.2. ^{13}C NMR (DMSO-d_6, 100 MHz):

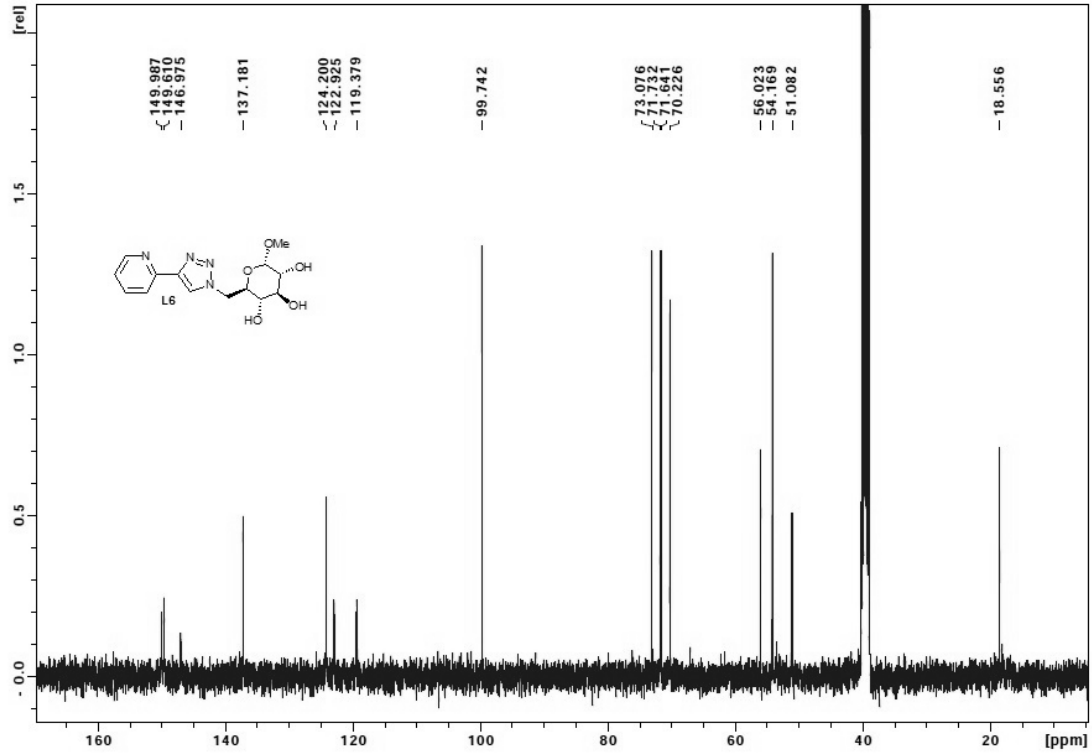

2.4. Ligand **L7**

2.4.1. ^{1}H NMR (DMSO-d_6, 400 MHz):

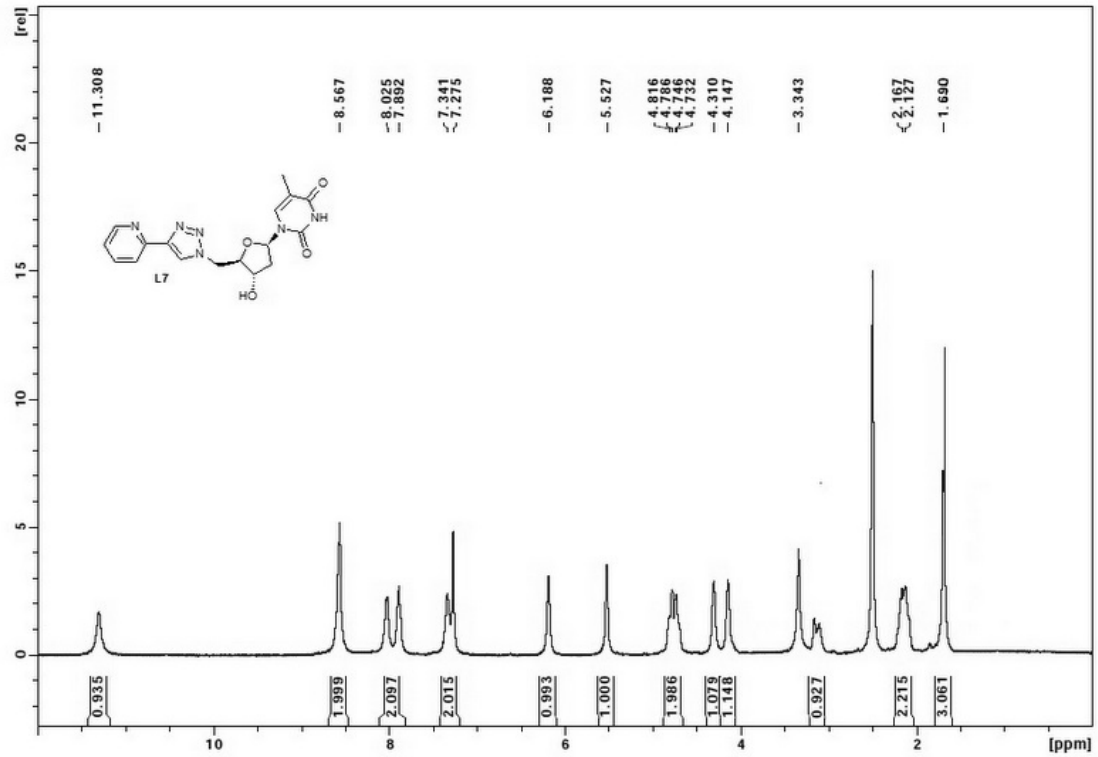

2.4.2. ^{13}C NMR (DMSO-d_6, 100 MHz):

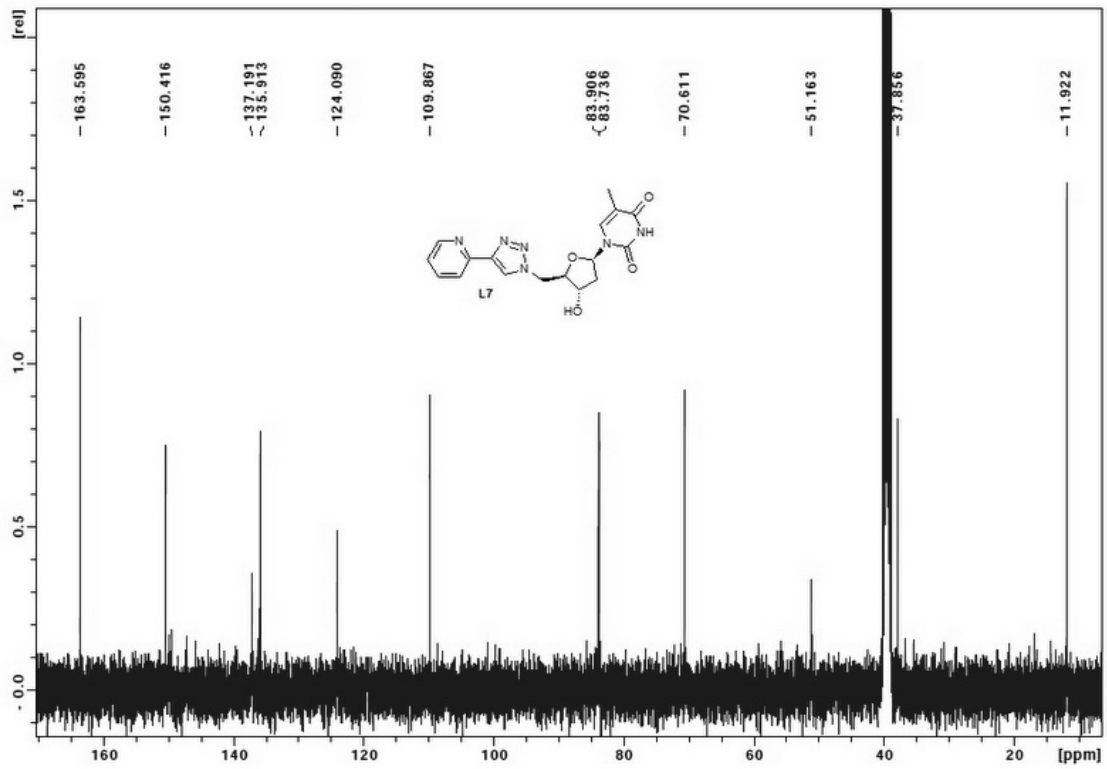

2.5. Ligand **L8**

2.5.1. ^{1}H NMR (DMSO-d_6, 400 MHz):

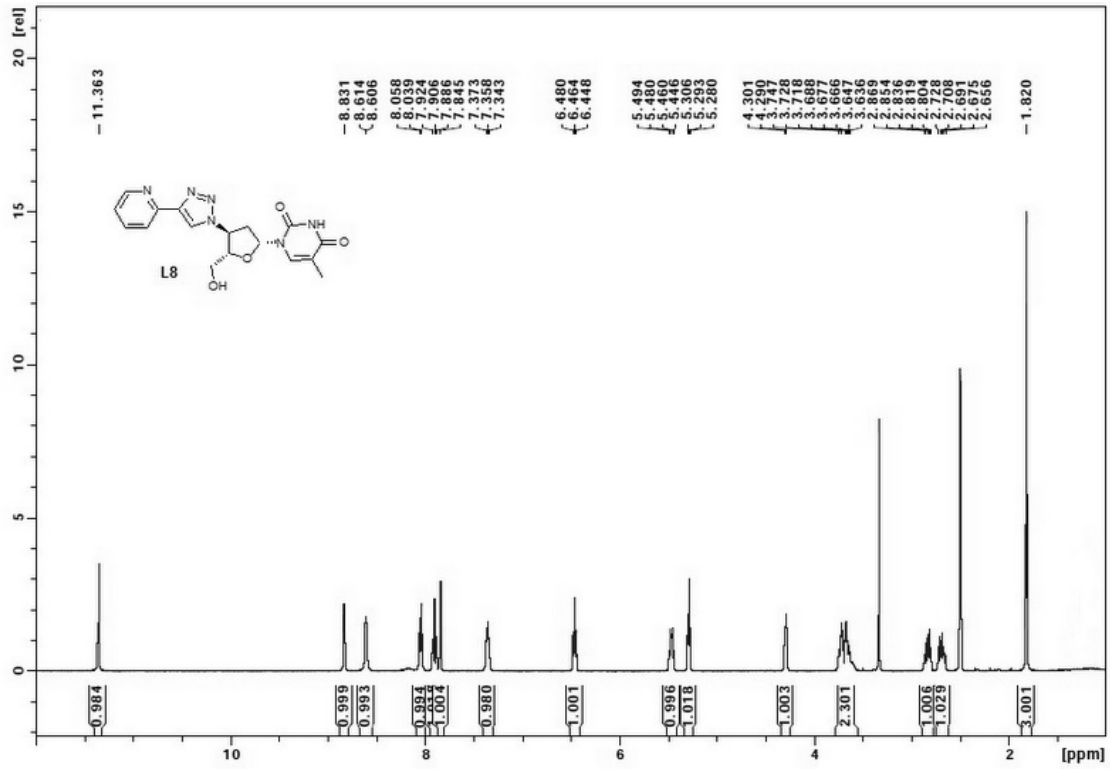

2.5.2. ^{13}C NMR (DMSO-d_6, 100 MHz):

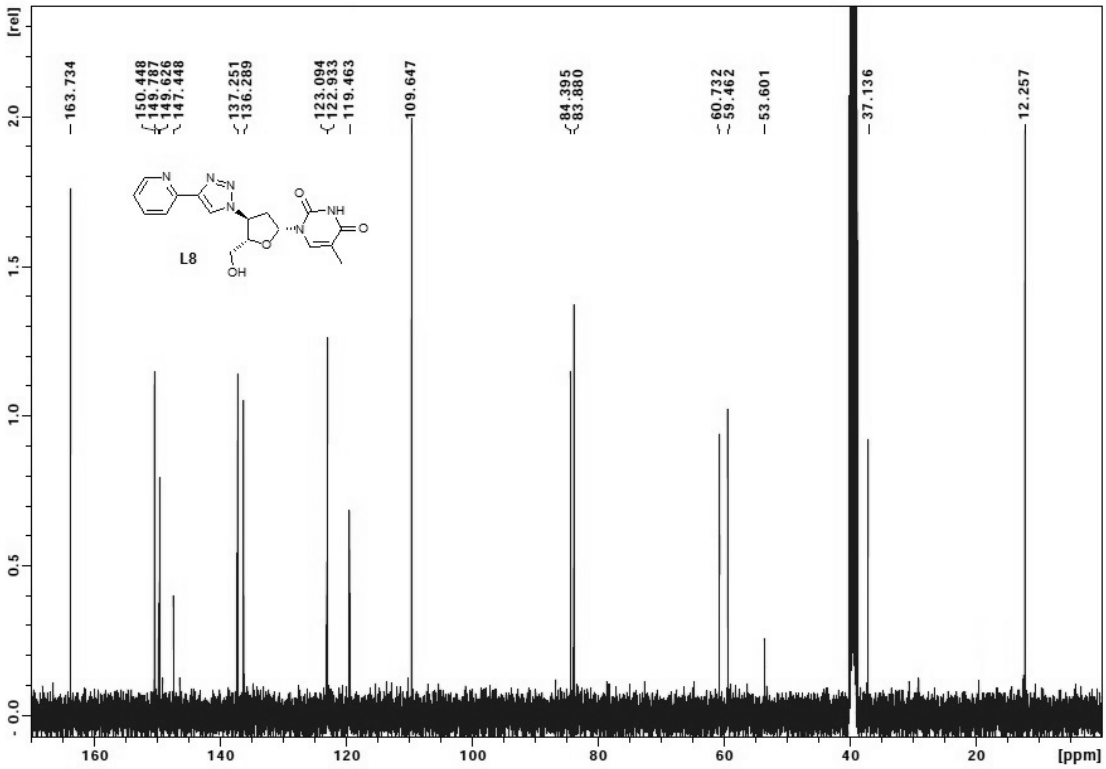

2.6. Compound **1Ru**

2.6.1. ^{1}H NMR (DMSO-d_6, 400 MHz):

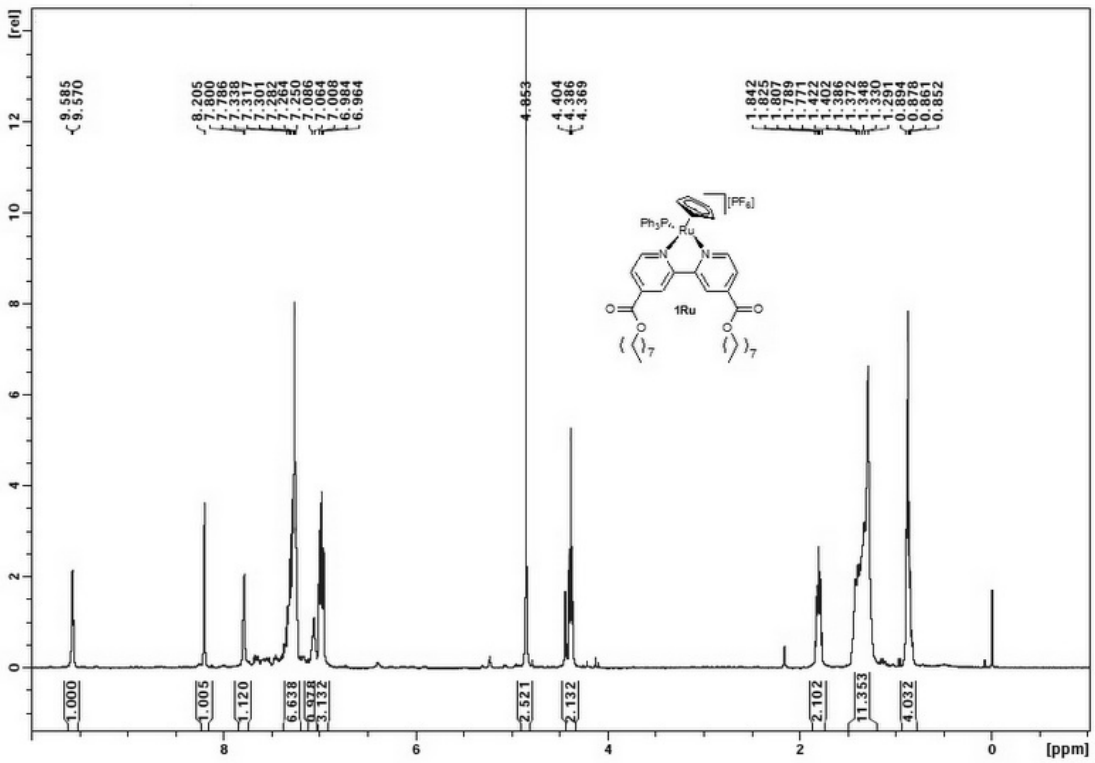

2.6.2. ^{13}C NMR (DMSO-d_6, 100 MHz):

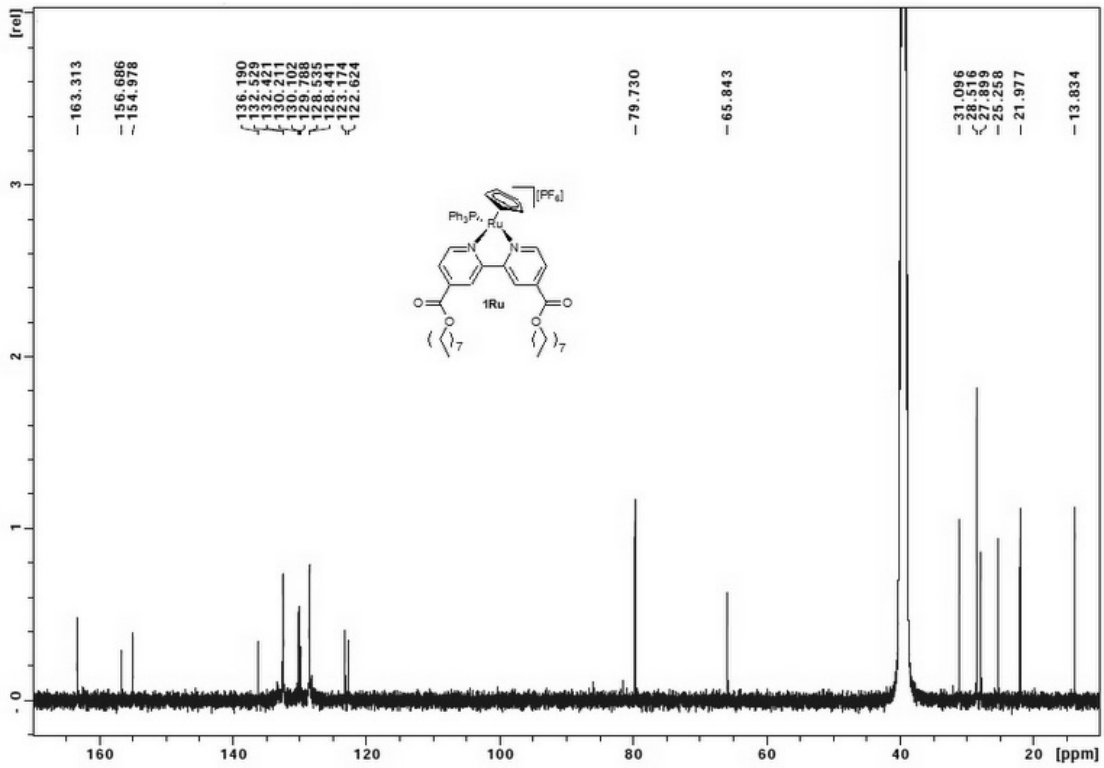

2.6.3. ^{31}P NMR (DMSO-d_6, 162 MHz):

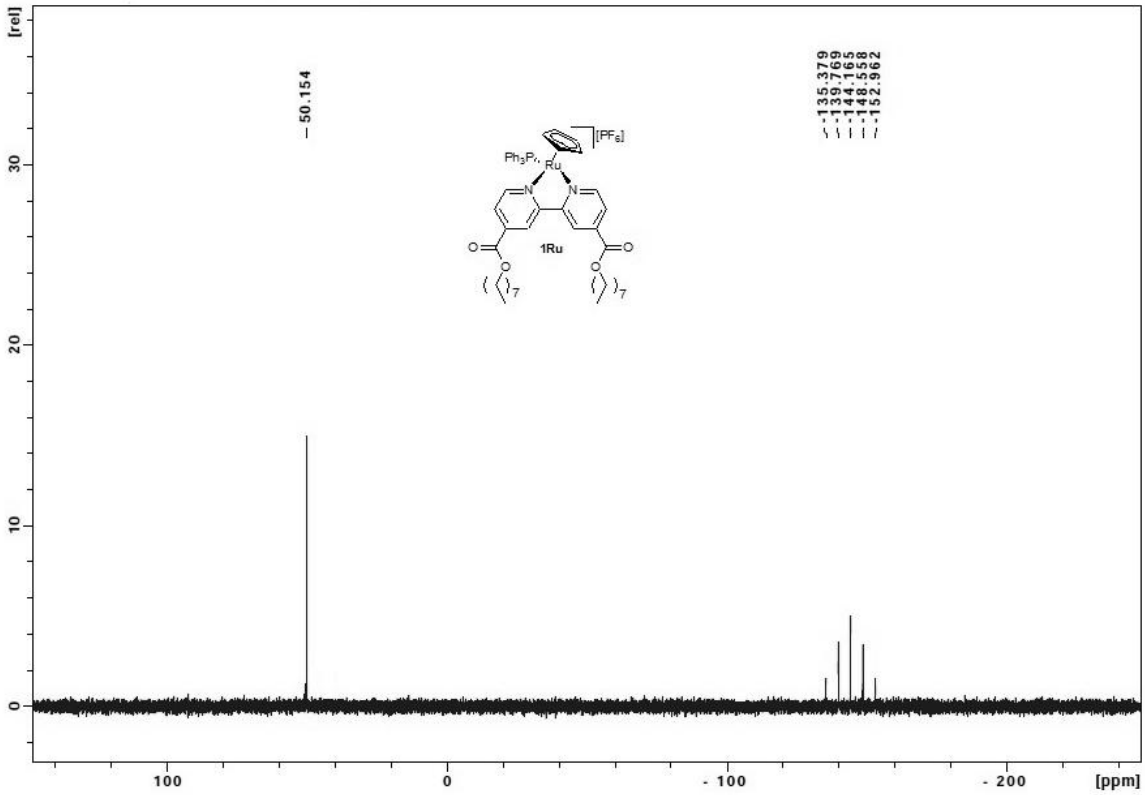

2.7. Compound **2Ru**

2.7.1. ^{1}H NMR (DMSO-*d6*, 400 MHz):

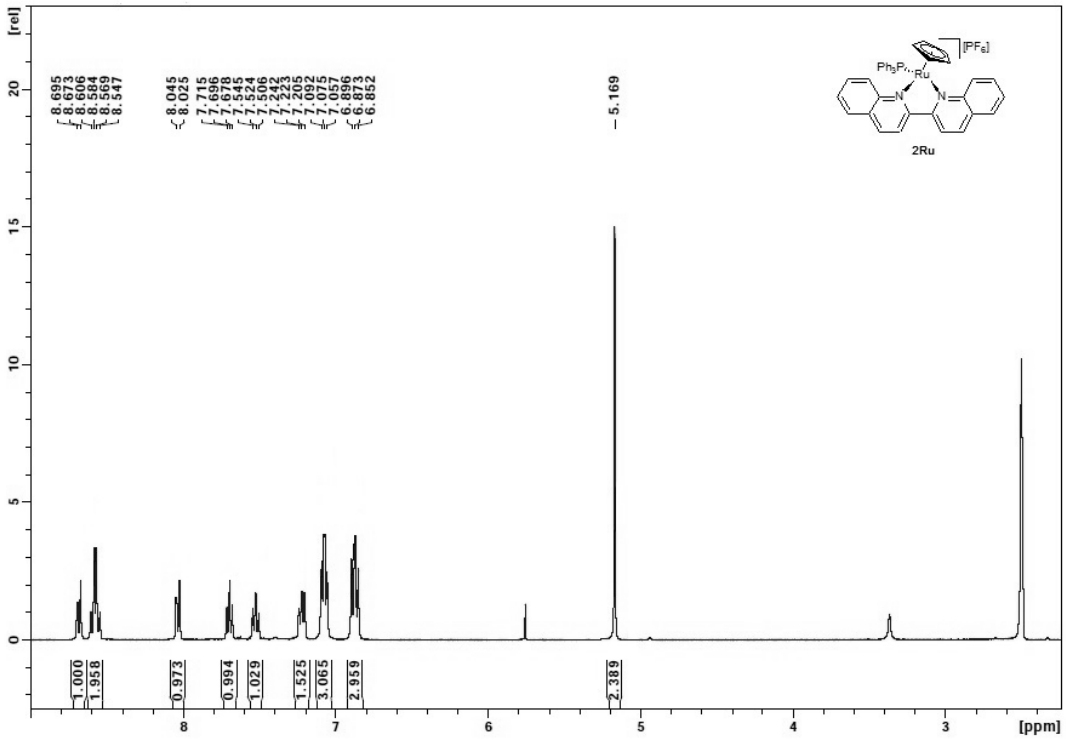

2.7.2. ^{13}C NMR (DMSO-d_6, 100 MHz):

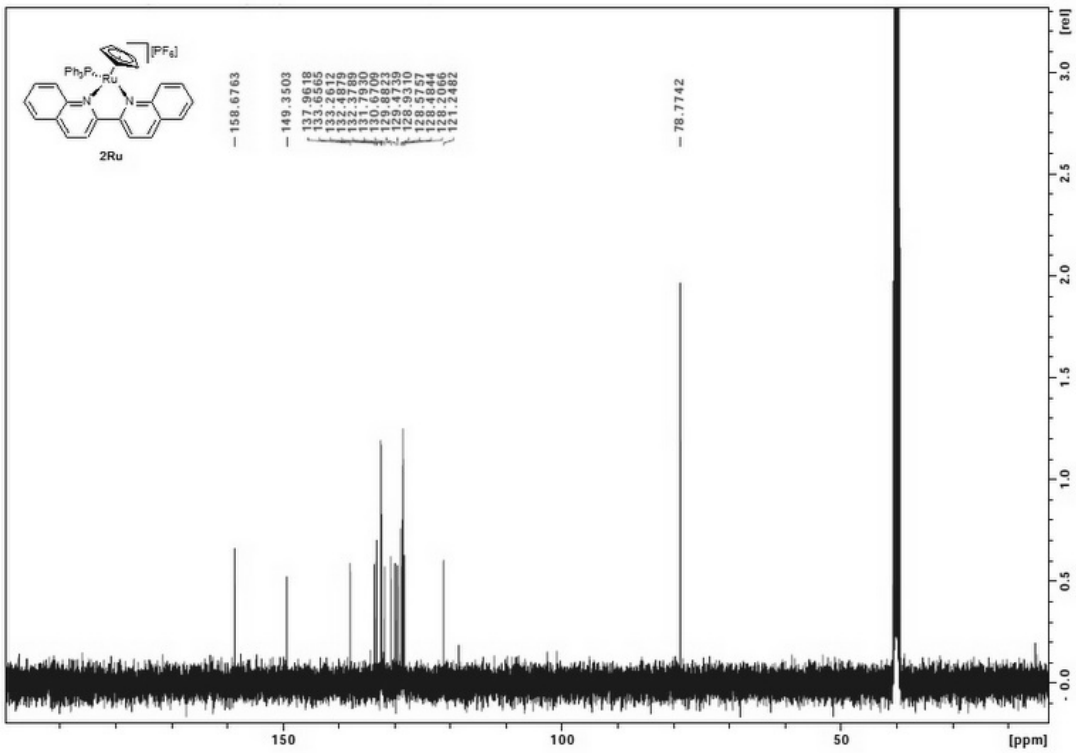

2.7.3. ^{31}P NMR (DMSO-d_6, 162 MHz):

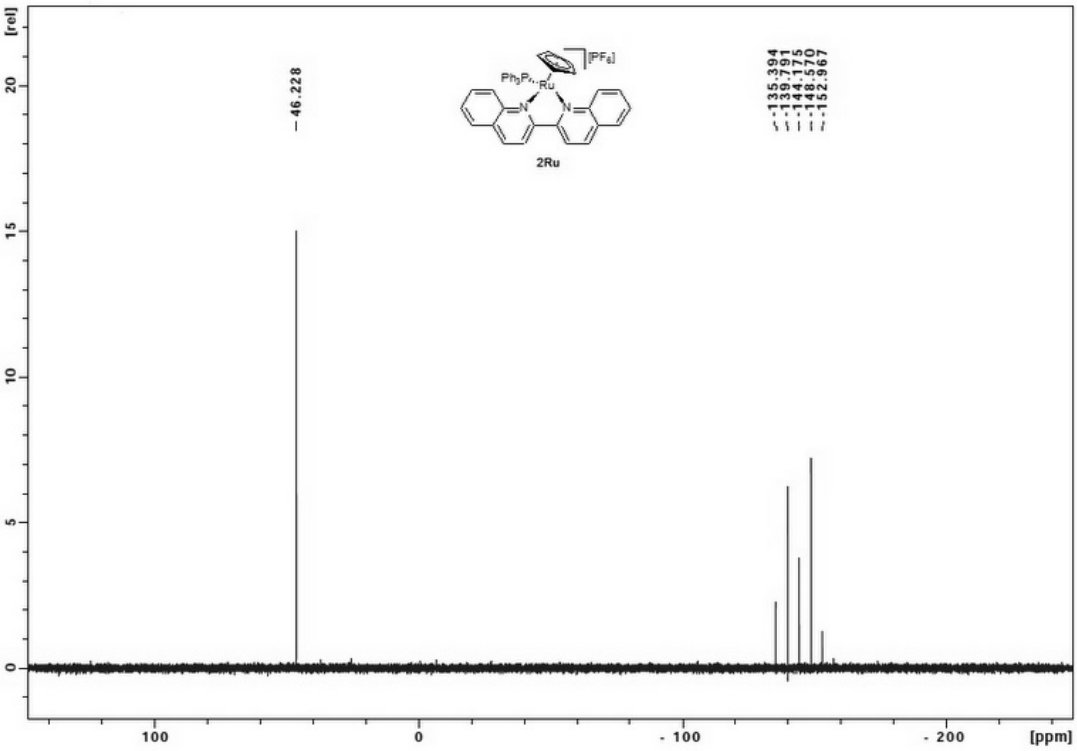

2.8. Compound **3Ru**

2.8.1. ^{1}H NMR (DMSO-d_6, 400 MHz)

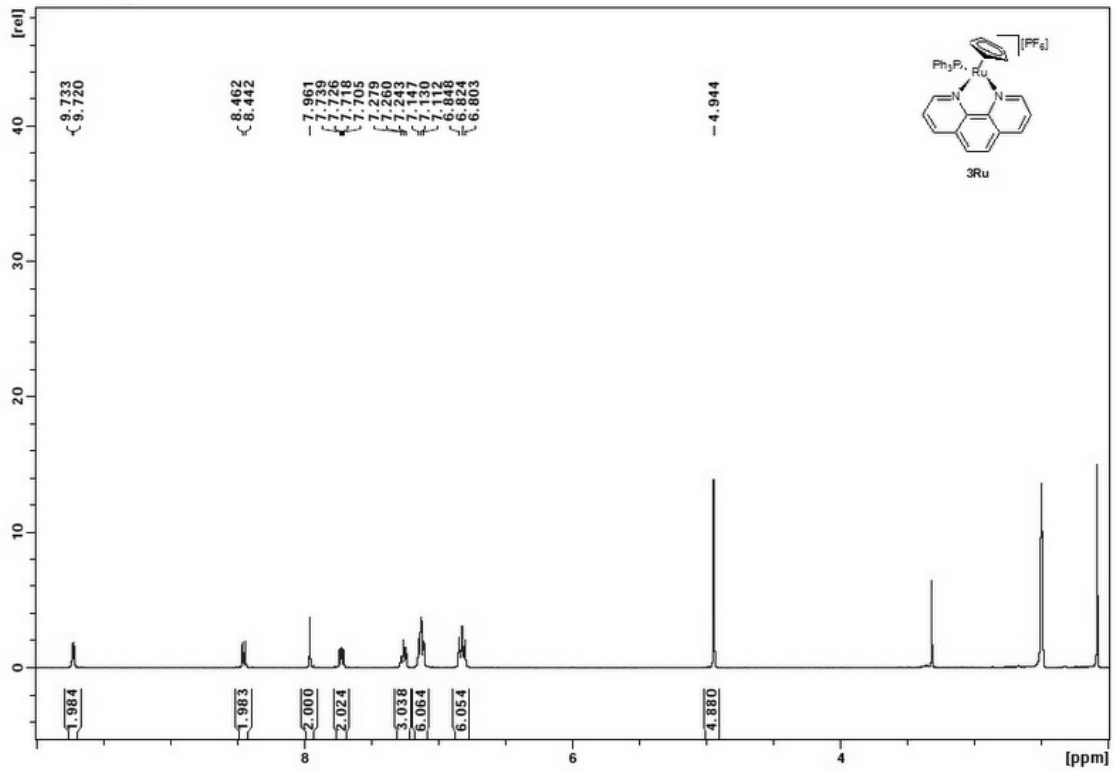

2.8.2. ^{13}C NMR (DMSO-d_6, 100 MHz):

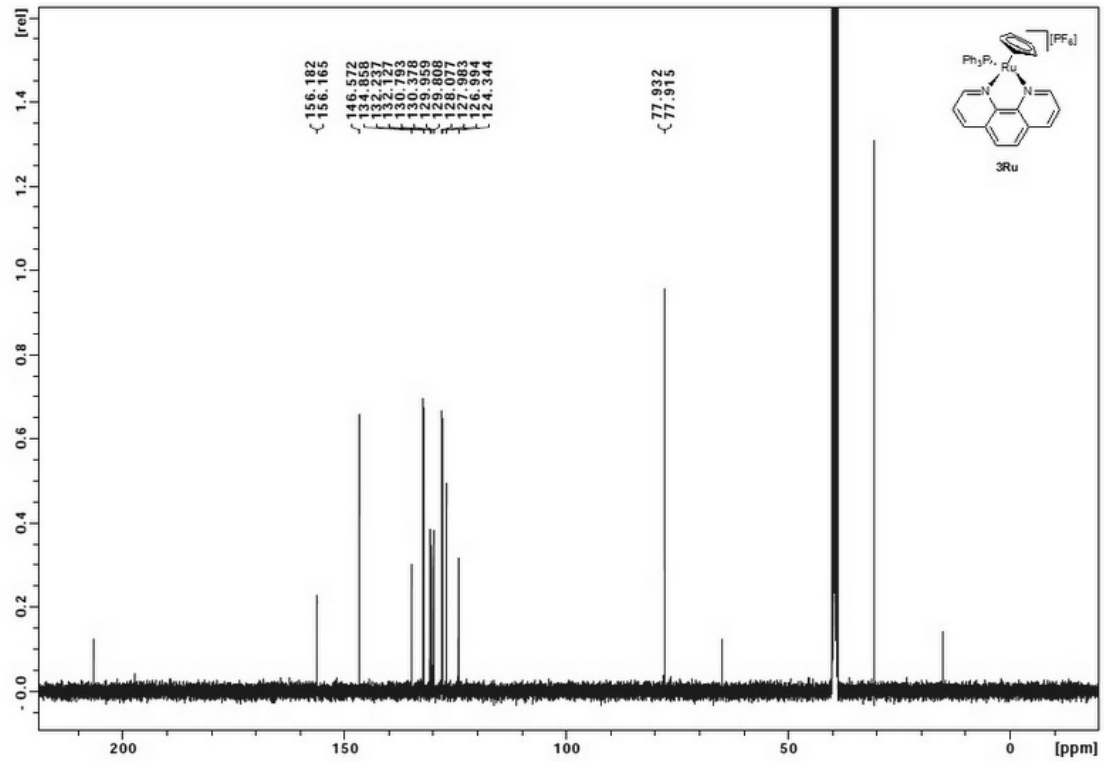

2.8.3. ^{31}P NMR (DMSO-$_{d6}$, 162 MHz):

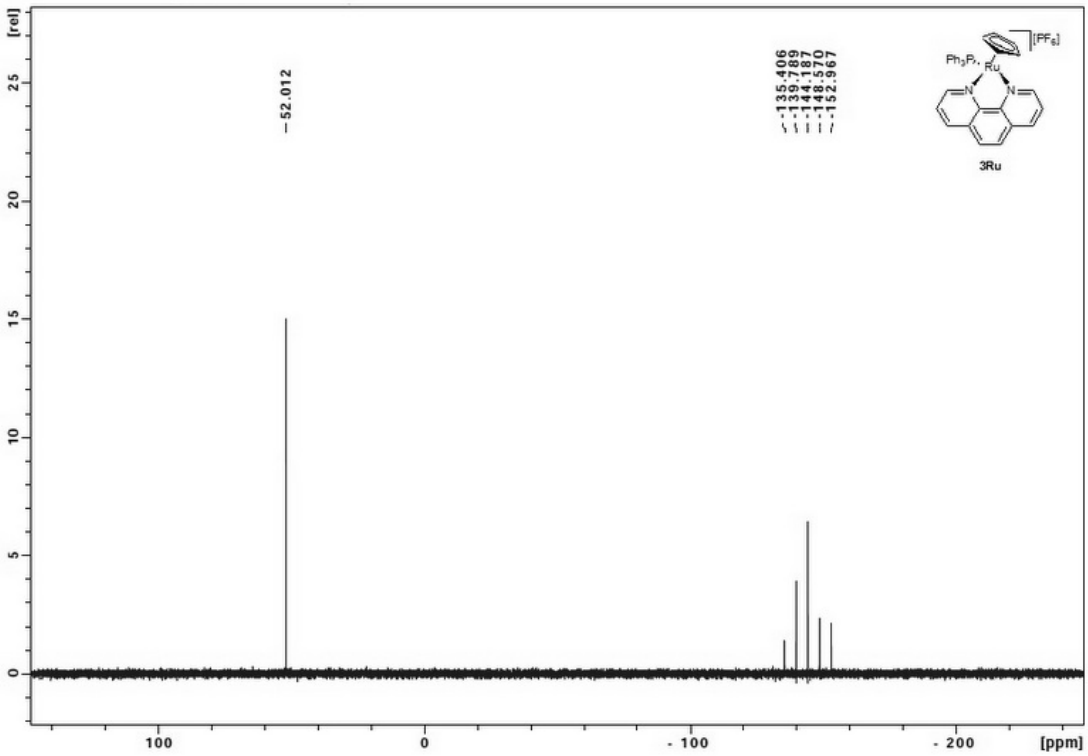

2.9. Compound **4Ru**

2.9.1. ^{1}H NMR (DMSO-d_6, 400 MHz):

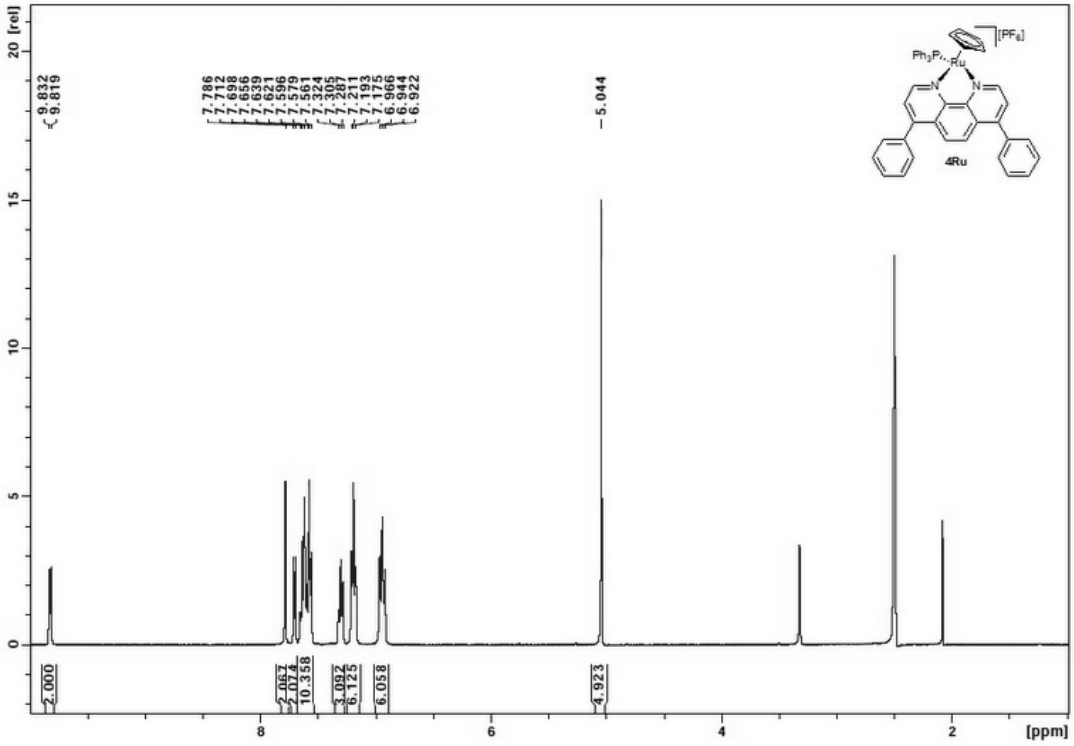

2.9.2. ^{13}C NMR (DMSO-d_6, 100 MHz):

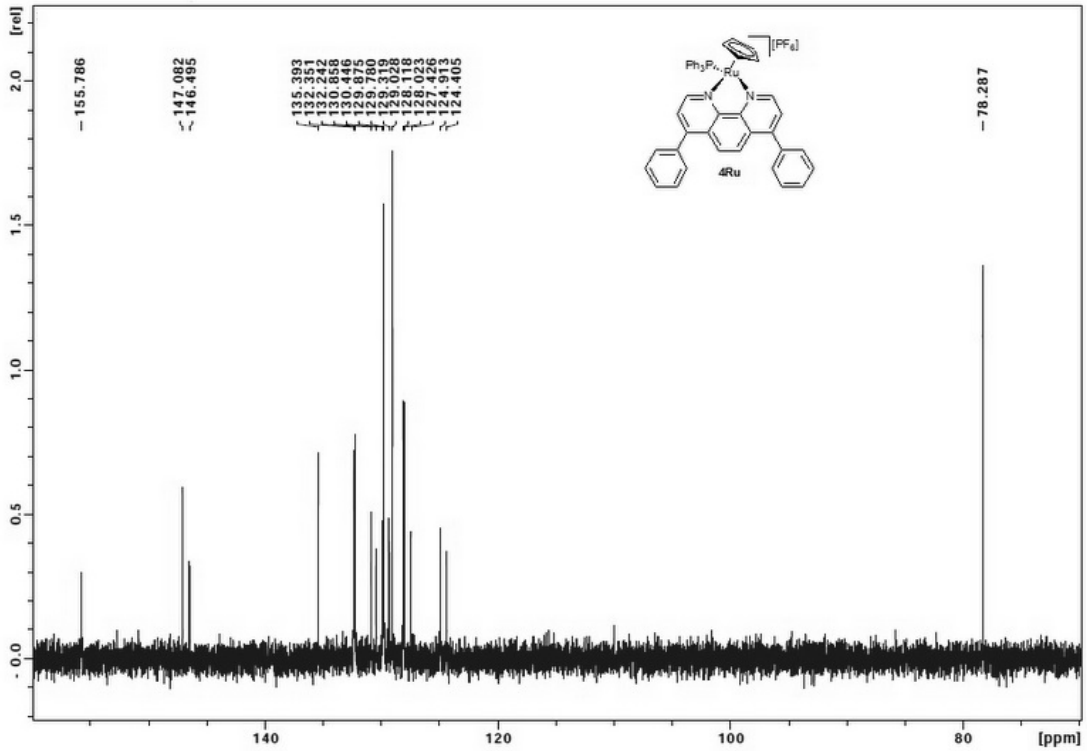

2.9.3. ^{31}P NMR (DMSO-d_6, 162 MHz):

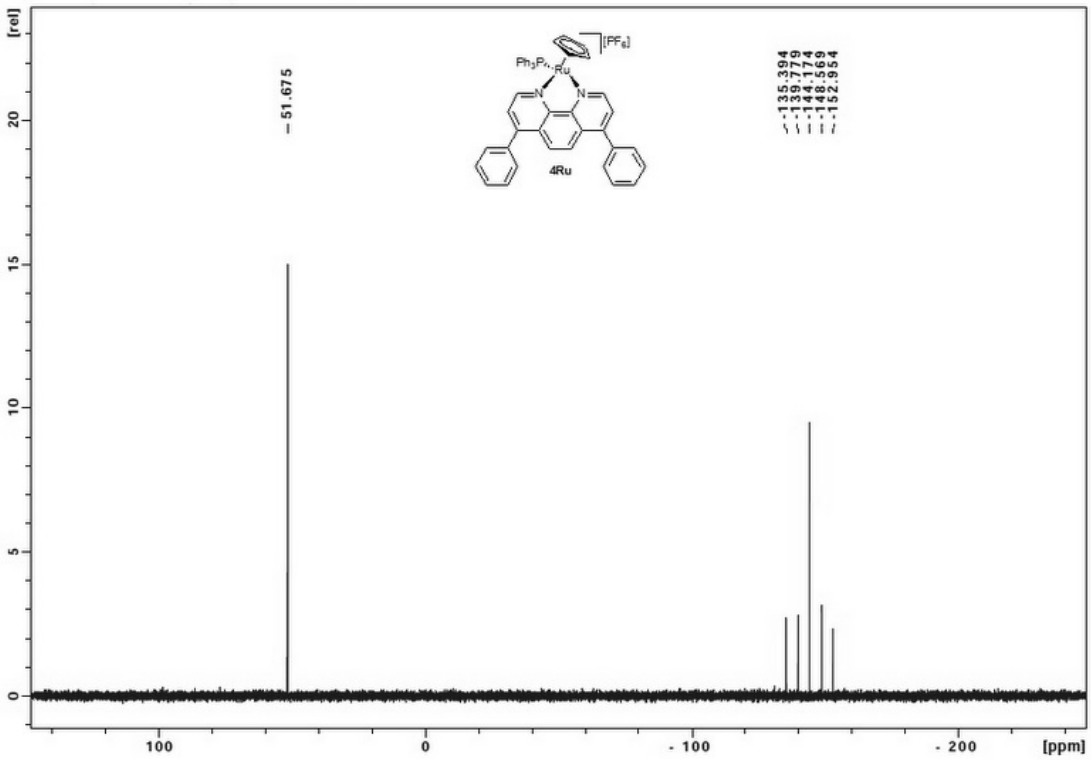

3. ESI spectra of compounds **5Ru-8Ru**.

3.1. Compound **5Ru**:

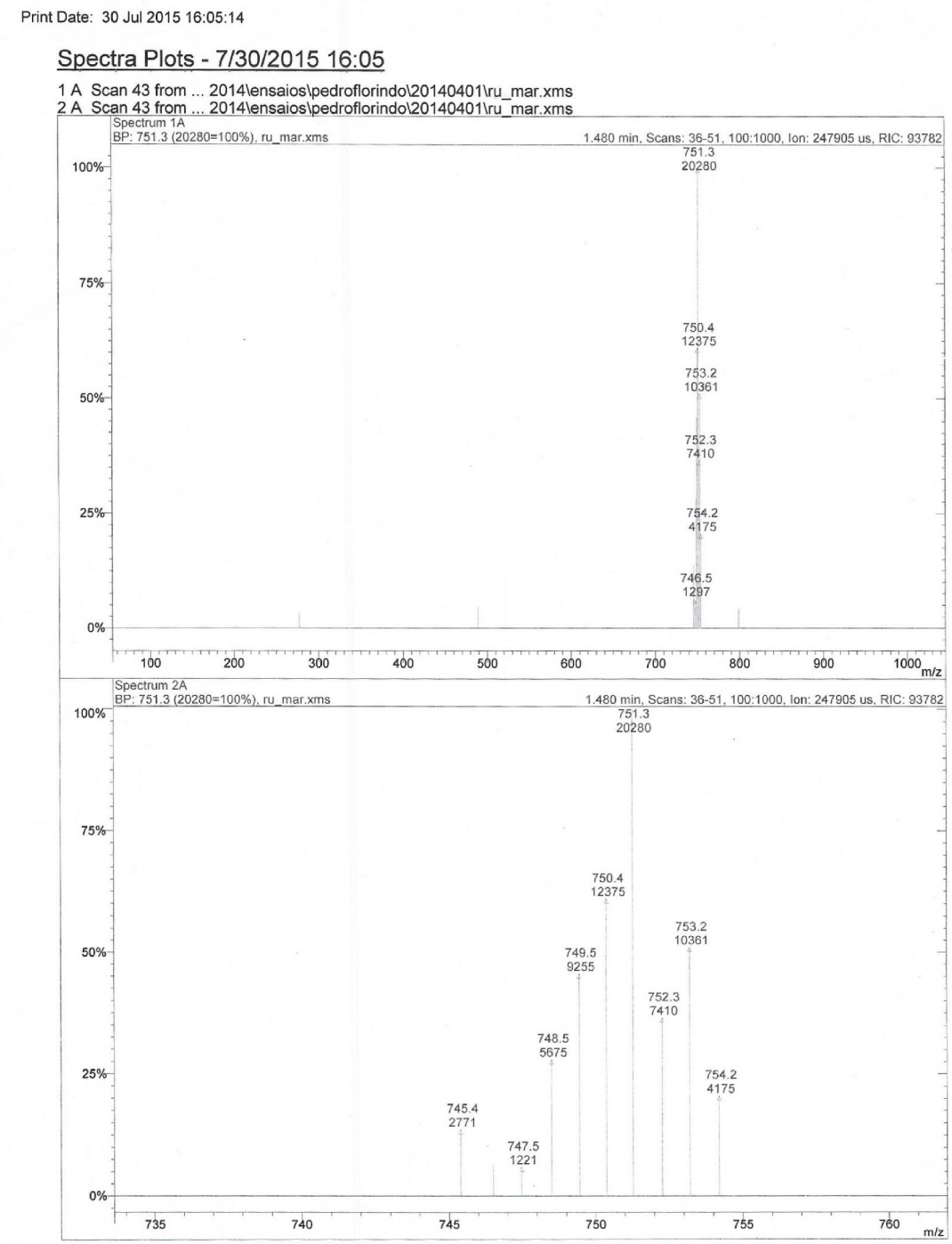

3.2. Compound **6Ru**:

Print Date: 30 Jul 2015 16:05:51

Spectra Plots - 7/30/2015 16:05

1 A Scan 20 from ... 2014\ensaios\pedroflorindo\20140401\ru_glu.xms
2 A Scan 20 from ... 2014\ensaios\pedroflorindo\20140401\ru_glu.xms

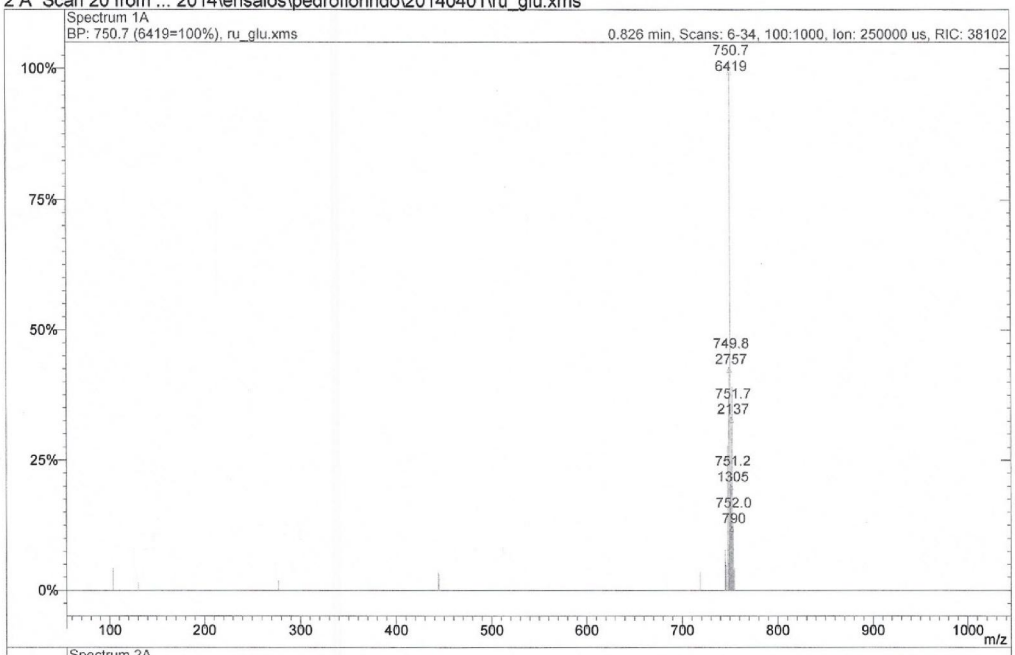

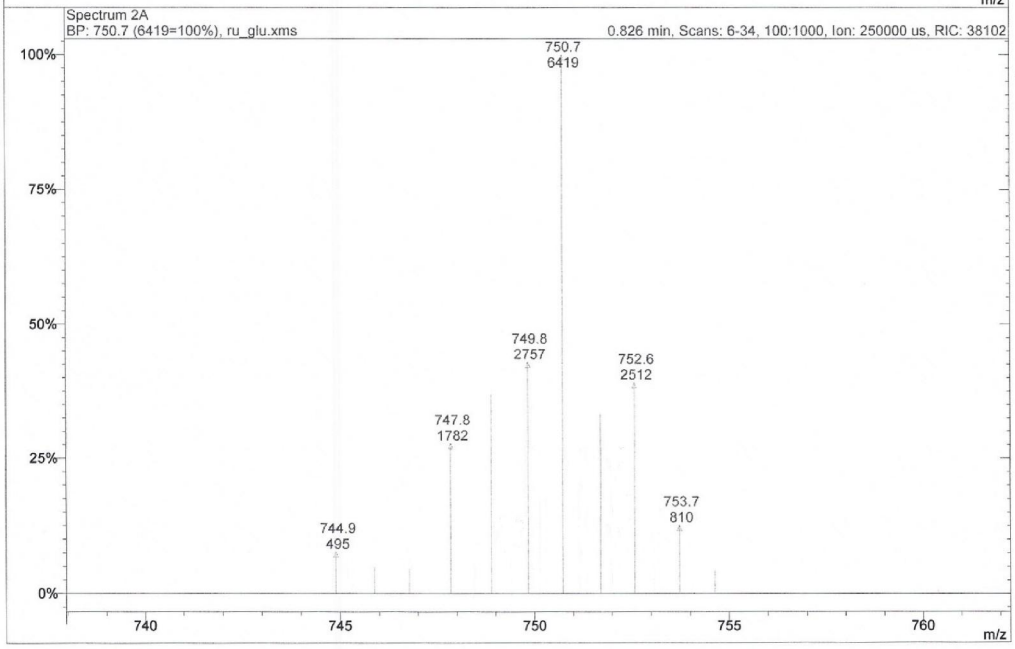

3.3. Compound **7Ru**:

Print Date: 30 Jul 2015 16:07:36

Spectra Plots - 7/30/2015 16:07

1 A Scan 18 from ...o 2014\ensaios\pedroflorindo\20140331\ruthy.xms
2 A Scan 18 from ...o 2014\ensaios\pedroflorindo\20140331\ruthy.xms

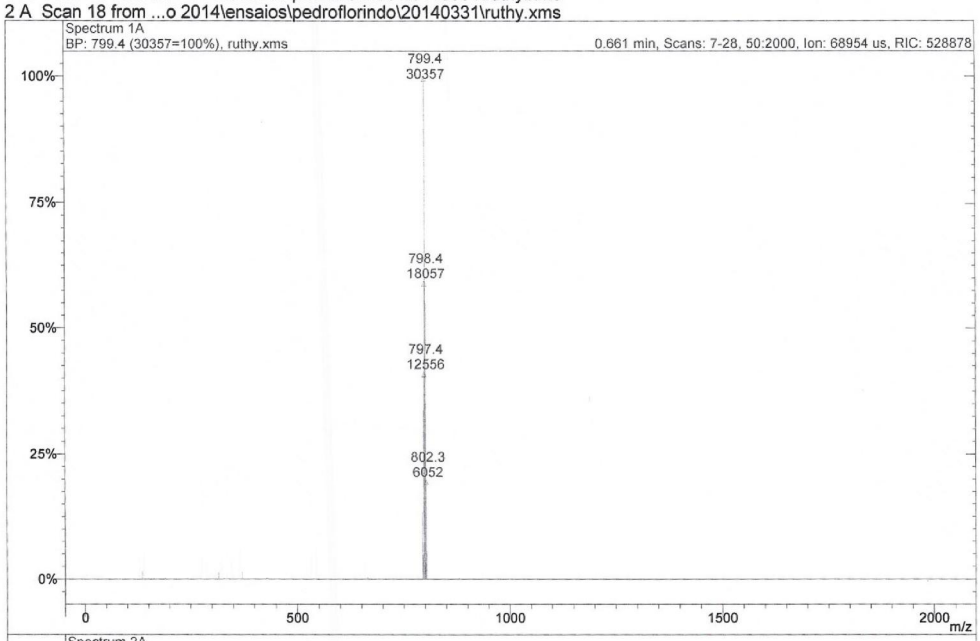

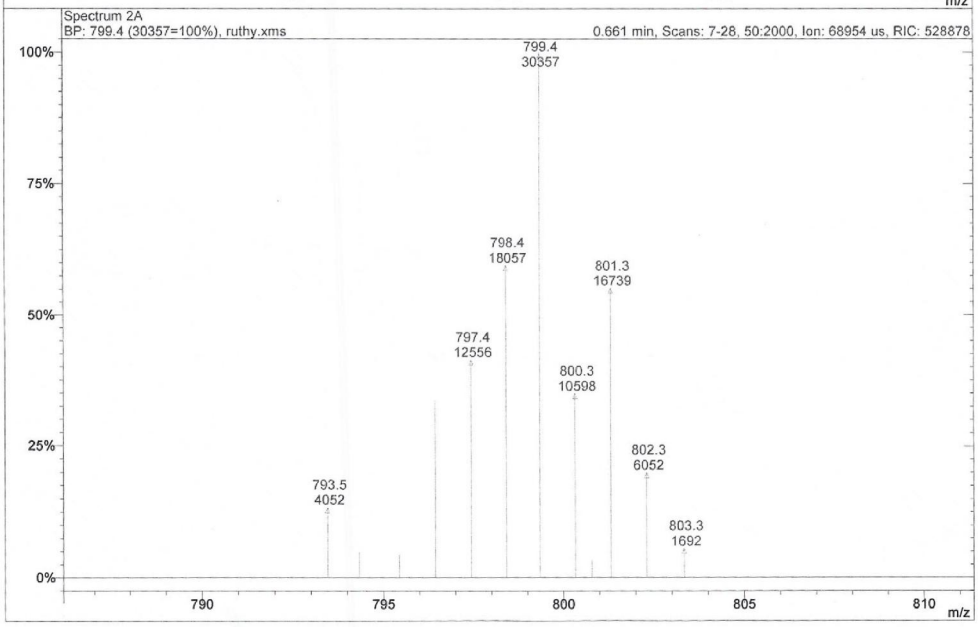

3.4. Compound **8Ru**:

Print Date: 30 Jul 2015 16:06:32

Spectra Plots - 7/30/2015 16:06

1 A Scan 41 from ... 2014\ensaios\pedroflorindo\20140401\ru_azt.xms
2 A Scan 41 from ... 2014\ensaios\pedroflorindo\20140401\ru_azt.xms

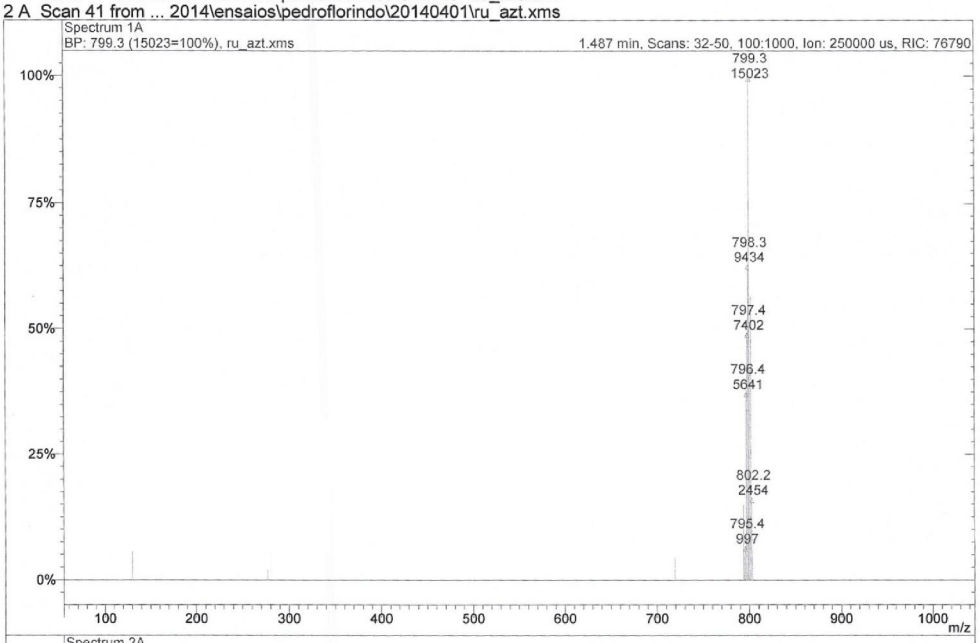

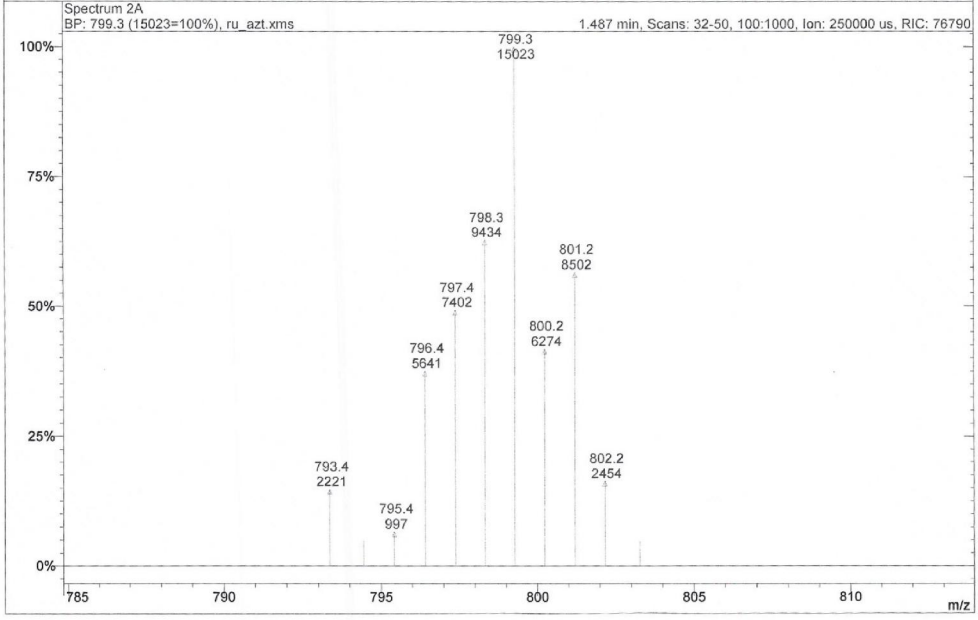

4. X-ray crystallographic data for compounds **2Ru-4Ru**

Suitable crystals for X-ray diffraction studies were obtained by slow diffusion of n-hexane in dichloromethane (**2Ru, 3Ru**) or diethyl ether in acetone (**4Ru**) solutions of the compounds, and mounted with protective oil on a cryo-loop. X-ray single diffraction was conducted on Bruker D8 and X8 Apex II diffractometers equipped with MoKα X-ray sources and graphite monochromators. The X-ray generators were operated at 50 kV and 30 mA and the X-ray data collection were monitored using the APEX2 program.[4] Multiscan absorption correction was applied using SAINT and SADABS programs.[4] Structures were solved by direct methods with the program SHELXS97[5] and refined by full-matrix least squares on F^2 with SHELXL97,[6] both included in the package of programs WINGX-V2014.1.[7] Non-hydrogen atoms were refined with anisotropic thermal parameters, with H-atoms placed in idealized positions and allowed to refine riding on the parent C atom. The CH_2Cl_2 molecule in **3Ru** is disordered, and was modelled. **2Ru** crystal diffracted poorly, with a low resolution. PLATON[8] was used to calculate bond distances and angles as well as hydrogen bond interactions. Graphical representations were prepared using Mercury 3.5.1.[9] Molecular structures of the complexes are shown in Figure S1 and selected bond lengths and angles presented in Table S1.

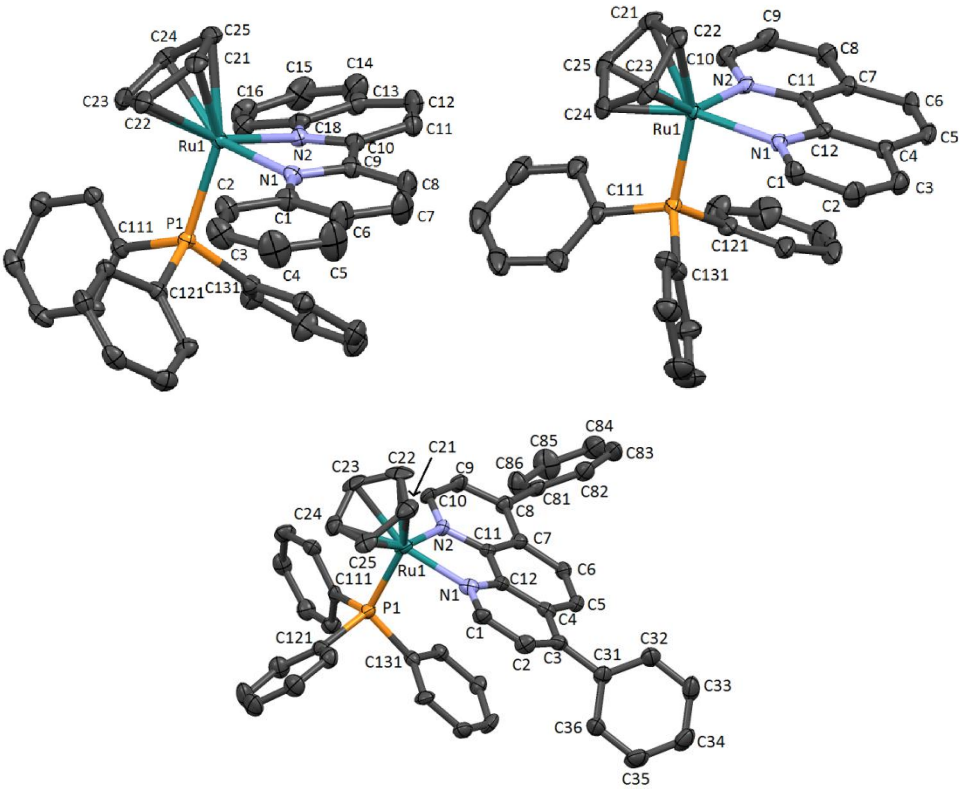

Figure S1. Crystal structure of monocationic complexes **2Ru**, **3Ru** and **4Ru**, with atom labelling. Displacement ellipsoids are drawn at 50% probability level; hydrogens are omitted for picture clarity.

Table S1. Selected bond distances (Å) and angles (º).

Compound	**2Ru**	**3Ru**	**4Ru**
Bond Lenghts (Å)			
Ru-(η^5-C_5H_5)[a]	1.8399(2)	1.8247(3)	1.8294(5)
Ru-N(1)	2.117(2)	2.095(3)	2.085(5)
Ru-N(2)	2.120(2)	2.081(3)	2.095(5)
Ru-P	2.3277(6)	2.3002(11)	2.316(2)
Angles (º)			
(η^5-C_5H_5)[a]-M-N(1)	125.40(5)	131.34(9)	129.42(15)
(η^5-C_5H_5)[a]-M-N(2)	125.71(5)	126.99(9)	130.16(14)
(η^5-C_5H_5)[a]-M-P	127.354(16)	125.48(3)	125.82(5)
N(1)-M-P	93.70(5)	88.48(9)	90.4(2)
N(2)-M-P	93.91(5)	92.14(10)	88.4(2)
N(1)-M-N(2)	76.51(4)	77.79(13)	77.1(2)

[a]Centroid.

Compounds **2Ru** and **3Ru** crystallize in triclinic crystal system, space group P-1, and compound **4Ru** in monoclinic crystal system, space group $P2_1/c$; compound **3Ru** crystalizes with a CH_2Cl_2 molecule. All compounds present the usual "three-legged piano stool" distribution of the ligands around the metal centre, with N-N ligands as "double-legs". Complex **2Ru**, with 2,2'-biquinoline ligand, presents longer Ru-L distances (L= $Cp^{centroid}$, N-N, PPh_3) than phenanthroline analogs **3Ru** and **4Ru**. Despite symmetry of bidentate N-N ligands, all complexes have different Ru-N bond distances. N-Ru-N angles are slightly larger for **3Ru** and **4Ru** than for **2Ru**, due to the structural rigidity imposed by ortho-fused phenanthroline ligands. This is also reflected in the *quasi*-planarity of phenanthroline ring systems, while the biquinoline in **2Ru** is much less planar: the angle between the planes of the two quinoline rings is 14.3º, while in the ortho-fused phenanthrolines is less than 2.4º.

CCDC 1444128-1444130 contains the supplementary crystallographic data for this paper (**3Ru, 4Ru** and **2Ru**, respectively). These data can be obtained free of charge via www.ccdc.cam.ac.uk/data_request/cif, by emailing data_request@ccdc.cam.ac.uk or by contacting The Cambridge Crystallographic Data Centre, 12, Union Road, Cambridge CB2 1EZ, UK; fax +44 1223 336033.

5. Cell culture.

HCT116 human colon carcinoma cells were grown in McCoy's 5A modified medium supplemented with 10 % heat-inactivated fetal bovine serum (FBS) and 1 % antibiotic/antimycotic solution (Gibco, Life Technologies, Paisley, UK), and cultured at 37 °C under a humidified atmosphere of 5 % CO_2. Cells were seeded in 96-well plates, at 10^4 cells/well for dose-response curves and inhibition experiments.

6. Cell treatments

Stock solutions of organometallic compounds **1Ru-8Ru** and TM34[PF_6] were prepared in sterile DMSO. Prior to all treatments, cells were allowed to adhere for 24 h, and then exposed to test compounds for the indicated times. To plot dose-response curves, cells were exposed to 0.1–100 μM test compounds for 72 h. Oxaliplatin, a cytotoxic agent used in colon cancer treatment, was used as a positive control. For uptake competition experiments, organometallic compounds were tested at IC_{50} and 2-fold IC_{50} concentrations for 72 h. To block GLUT-mediated transport, cells were treated with carbohydrate derivative compounds in MEM medium (5 mM D-glucose) supplemented with GlutaMAX (Gibco), 10 % FBS and 1 % antibiotic/antimycotic solution, in the presence or absence of 50 mM D-glucose/L-glucose. To block NT-mediated cellular uptake, cells were treated with 200 μM 2′-deoxyadenosine or 10 μM dipyridamole in combination with the nucleoside derivative compounds. All experiments were performed in parallel with DMSO vehicle control. The final DMSO concentration was always 0.1 %.

7. Viability assays

Cell viability was evaluated using the CellTiter 96 AQ_{ueous} Non-Radioactive Cell Proliferation Assay (Promega, Madison, WI, USA), according to the manufacturer's instructions. This colorimetric assay is based on the bio-reduction of 3-(4,5-dimethylthiazo-2-yl)-5-(3-carboxymethoxyphenyl)-2-(4-sulfophenyl)-2H-tetrazolium inner salt (MTS) to formazan by dehydrogenase enzymes found within metabolically active cells. The amount of water soluble formazan product can be measured by the amount of 490 nm absorbance, correlating with the number of living cells in culture. For this purpose, changes in absorbance were assessed using a Model 680 microplate reader (Bio-Rad, Hercules, CA, USA). For dose-response experiments, best-fit IC_{50} values from at least three independent experiments were calculated using GraphPad Prism software (version 5.00; San Diego, CA, USA), using the log (inhibitor) *vs* response (variable slope) function.

8. Molecular docking

Complex **6Ru** was the most cytotoxic amongst the carbohydrate derivative complexes and since it is obtained as a diasterioisomeric mixture, 3D models of both diastereoisomers of **6Ru** were built and geometry optimized using the Gaussian09 package[10] at the PBE1PBE level of theory.[11] Given the cationic nature of these complexes, geometry optimization was performed in water using the Polarizable Continuum Model (PCM) using the integral equation formalism variant (IEFPCM)[12] as implemented in the software. The standard 6-31G* basis set was used for all elements except ruthenium and phosphorus for which the LANL2TZ(f) basis set with the associated effective core potential was employed.[13] The optimized structures are depicted in Figure S2.

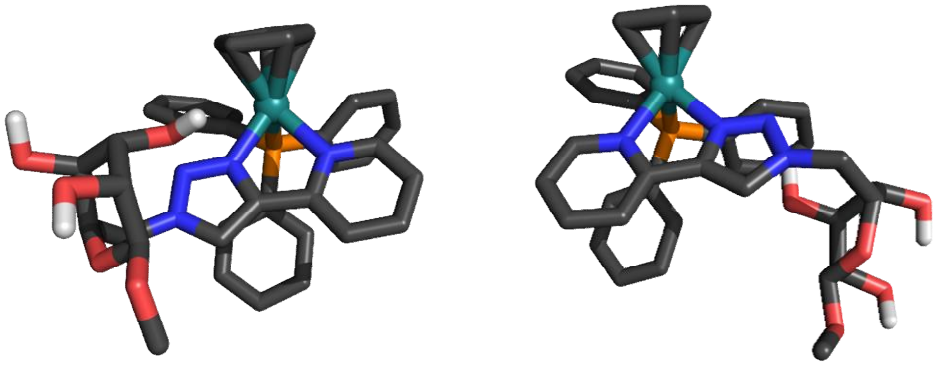

Figure S2. PBE1PBE optimized geometries of both diastereoisomers of **6Ru**: **6Ru'** (left) and **6Ru''** (right). Non-polar hydrogens were omitted for clarity.

The DFT optimized structure was converted to the PDBQT file *via* the Autodock graphical interface AutoDockTools[14] and in this process, non-polar hydrogen atoms were removed.

The crystal structure of the xylose transporter (XylE) from *Escherichia coli* bound to D-glucose was used as the receptor model. This structure was solved in an outward-open conformation thus providing a reasonable initial model for the scenario a given molecule encounters when entering a cell. Additionally, most of the important amino acids responsible for recognition of D-glucose are invariant in GLUT1.[15] In contrast, the structure of the human GLUT1 presents the inward open configuration[16] and, when aligned with XylE, significant steric clashes could be observed for the docking poses of some glucose–platinum conjugate complexes.[17]

The coordinates of XylE were retrieved form the RCSB Protein Data Bank (PDB code: 4GBZ)[15] and striped of water and co-crystalized α-D-glucose and β-nonylglucoside molecules. Missing heavy atoms in some residues were added in optimal positions with the LEaP utility from Ambertools.[18] The resultant PDB of the protein was also converted to the PDBQT format with AutoDockTools, removing the non-polar hydrogen atoms.

Molecular docking of **6Ru'** and **6Ru''** was performed using with the open-source program AutoDockVina 1.1.2.[19] Given that the ruthenium atom type is not available in AutoDockVina,

this atom was replaced by iron in the docking simulations. Since the metal is not directly exposed to the protein, being surrounded by bulky ligands in the coordination sphere, this approximation is acceptable and should not affect the docking results which are mainly dependent of the ligands.

The complexes have a substantial different geometric topology than D-glucose and preliminary rigid docking calculations showed that several protein side-chain atoms have steric clashes with the complexes, thus preventing a proper sampling of the binding cavity. In order to circumvent this problem, the side-chains of Phe24, Gln168, Gln175, Gln288, Asn294, Tyr298, Trp392, and Trp412 were considered flexible during the docking procedure. These residues were selected since they were shown to be important for D-glucose binding[15, 16] or because they presented significant clashes during the preliminary rigid docking experiments (not shown). The search space consisted on a box (27 × 27 × 27 Å) centered on the D-glucose binding site with an exhaustiveness criteria of 16. For each isomer, 100 independent docking runs were executed, each providing a minimum of 20 poses ranked according to the scoring function of AutodockVina. Both complexes are able to fit the binding cavity and in the lowest-energy binding poses, the $CpRu(PPh)_3$ core occupies the glucose-binding spot near Gln168, Gln288, Tyr298, and Gln175, key residues in glucose recognition (Fig. S4).

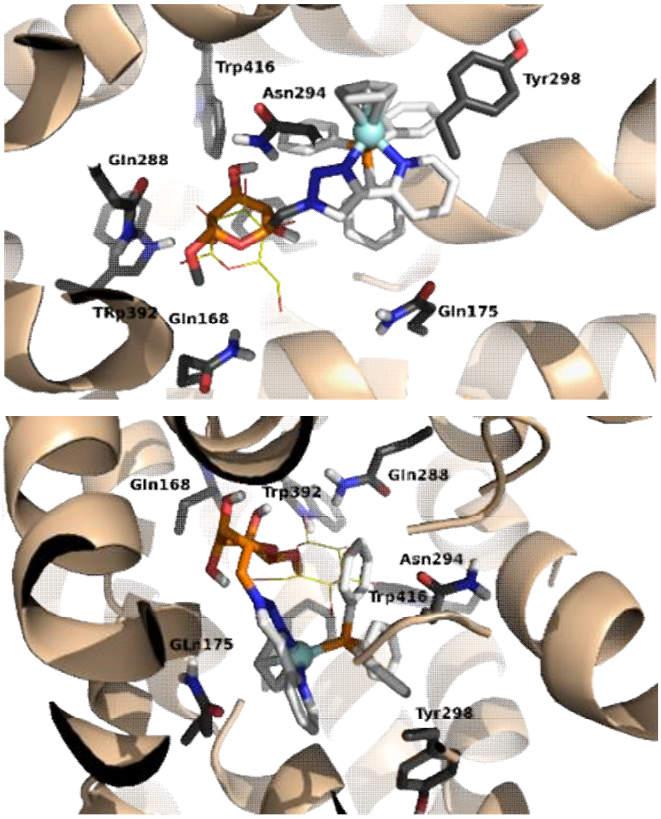

Figure S3. Complexes **6Ru'** (top) and **6Ru''** (bottom) docked into XylE (PDB 4GBZ) at glucose binding site. The protein is shown as cartoon with the flexible side chains depicted as

dark grey sticks. The sugar moieties are shown as orange sticks whereas the glucose in the X-ray structure is shown as yellow lines.

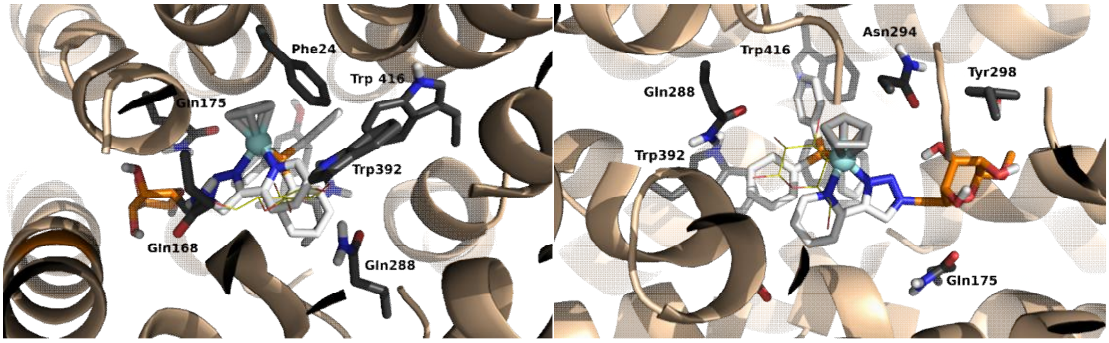

Figure S4. Most favorable binding poses for complexes **6Ru'** (left) and **6Ru''** (right) docked into XylE (PDB 4GBZ). The protein is shown as cartoon with the flexible side chains depicted as dark grey sticks. The sugar moiety in both complexes is shown as orange sticks whereas the glucose in the X-ray structure is shown as yellow lines.

8. References

(1) D. D. Perrin, W. L. F. Amarego and D. R. Perrin, Purification of Laboratory Chemicals, 2nd ed., Pergamon, New York, 1980.

(2) G. S. Ashby, M. I. Bruce, I. B. Tomkins and R. C. Walli, *Aust. J. Chem.*, 1979, **32**, 1003.

(3) A. Valente, M. H. Garcia, F. Marques, Y. Miao, C. Rousseau and P. Zinck, *J. Inorg. Biochem.*, 2013, **127**, 79.

(4) SABADS, Area-detector Absorption Correction, Bruker AXS Inc., Madison, WI, **2004**.

(5) G. M. Sheldrick, *Acta Cryst.*, **A64**, 2008, 112.

(6) G. M. Sheldrick, SHELXL-97: An integrated system for solving and refining crystal structures from diffraction data (Revision 5.1). University of Göttingen, Germany, **1997**.

(7) L. J. Farrugia, *J. Appl. Cryst.*, **32**, 1999, 837.

(8) A. L. Spek, *Acta Crystallogr.*, **D65**, 2009, 148.

(9) C. F. Macrae, P. R. Edgington, P. McCabe, E. Pidcock, G. P. Shields, R. Taylor, M.Towler and J. Van de Streek, *J. Appl. Cryst.*, **39**, 2006, 453.

(10) Gaussian 09, Revision A.02, M. J. Frisch, G. W. Trucks, H. B. Schlegel, G. E. Scuseria, M. A. Robb, J. R. Cheeseman, G. Scalmani, V. Barone, B. Mennucci, G. A. Petersson, H. Nakatsuji, M. Caricato, X. Li, H. P. Hratchian, A. F. Izmaylov, J. Bloino, G. Zheng, J. L. Sonnenberg, M. Hada, M. Ehara, K. Toyota, R. Fukuda, J. Hasegawa, M. Ishida, T. Nakajima, Y. Honda, O. Kitao, H. Nakai, T. Vreven, J. A. Montgomery, Jr., J. E. Peralta, F. Ogliaro, M. Bearpark, J. J. Heyd, E. Brothers, K. N. Kudin, V. N. Staroverov, R. Kobayashi, J. Normand, K. Raghavachari, A. Rendell, J. C. Burant, S. S. Iyengar, J. Tomasi, M. Cossi, N. Rega, J. M. Millam, M. Klene, J. E. Knox, J. B. Cross, V. Bakken, C. Adamo, J. Jaramillo, R. Gomperts, R. E. Stratmann, O. Yazyev, A. J. Austin, R. Cammi, C. Pomelli, J. W. Ochterski, R. L. Martin, K. Morokuma, V. G. Zakrzewski, G. A. Voth, P. Salvador, J. J. Dannenberg, S. Dapprich, A. D. Daniels, Ö. Farkas, J. B. Foresman, J. V. Ortiz, J. Cioslowski, and D. J. Fox, Gaussian, Inc., Wallingford CT, 2009.

(11) C. Adamo, V. Barone, *J. Chem. Phys.*, 1999, **110**, 6158.

(12) J. Tomasi, B. Mennucci, R. Cammi, *Chem. Rev.*, 2005, **105**, 2999.

(13) L. E. Roy, P. J. Hay, R. L. Martin, *J. Chem. Theory Comput.*, 2008, **4**, 1029.

(14) (a) G. M. Morris, R. Huey, W. Lindstrom, M. F. Sanner, R. K. Belew, D. S. Goodsell, A. J. Olson, *J. Comput. Chem.* 2009, **16**, 2785-91. (b) M. F. Sanner, *J. Mol. Graph. Model*, 1999, **17**, 57.

(15) L. Sun, X. Zeng, C. Yan, X. Sun, X. Gong, Y. Rao, N. Yan, *Nature*, 2012, **490**, 361.

(16) D. Deng, C. Xu, P. Sun, J. Wu, C. Yan, M. Hu, N. Yan, *Nature*, 2014, **510**, 121.

(17) M. Patra, T. C. Johnstone, K. Suntharalingam, S. J. Lippard, *Angew. Chem. Int. Ed.* 2016, **55**, 2550.

(18) D. A. Case, J. T. Berryman, R. M. Betz, D. S. Cerutti, T. E. Cheatham, III, T .A. Darden, R. E. Duke, T. J. Giese, H. Gohlke, A. W. Goetz, N. Homeyer, S. Izadi, P. Janowski, J. Kaus, A. Kovalenko, T. S. Lee, S. LeGrand, P. Li, T. Luchko, R. Luo, B. Madej, K. M. Merz, G. Monard, P. Needham, H. Nguyen, H. T. Nguyen, I. Omelyan, A. Onufriev, D. R. Roe, A. Roitberg, R. Salomon-Ferrer, C. L. Simmerling, W. Smith, J. Swails, R. C. Walker, J. Wang, R. M. Wolf, X. Wu, D. M. York, P.A. Kollman, AMBER 2015, University of California, San Francisco.

(19) O. Trott, A. J. Olson, *J. Comput. Chem.* 2010, **31**, 455.